Identifying the sources of uncertainty in climate model simulations of solar radiation modification with the G6sulfur and G6solar Geoengineering Model Intercomparison Project (GeoMIP) simulations

Daniele Visioni[1], Douglas G. MacMartin[1], Ben Kravitz[2,3], Olivier Boucher[4], Andy Jones[5], Thibaut Lurton[4], Michou Martine[6], Michael J. Mills[7], Pierre Nabat[6], Ulrike Niemeier[8], Roland Séférian[6], and Simone Tilmes[7]

[1]Sibley School for Mechanical and Aerospace Engineering, Cornell University, Ithaca, NY, USA
[2]Department of Earth and Atmospheric Science, Indiana University, Bloomington, IN, USA
[3]Atmospheric Sciences and Global Change Division, Pacific Northwest National Laboratory, Richland, WA, USA
[4]Institut Pierre-Simon Laplace, Sorbonne Université/CNRS, Paris, France
[5]Met Office Hadley Centre, Exeter, EX1 3PB, UK
[6]CNRM, Université de Toulouse, Meteo-France, CNRS, Toulouse, France
[7]Atmospheric Chemistry, Observations, and Modeling Laboratory, National Center for Atmospheric Research, Boulder, CO, USA
[8]Max Planck Institute for Meteorology, Hamburg, Germany

Correspondence: Daniele Visioni (dv224@cornell.edu)

Abstract. We present here results from the Geoengineering Model Intercomparison Project (GeoMIP) simulations for the experiment G6sulfur and G6solar for six Earth System Models participating in the Climate Model Intercomparison Project (CMIP) Phase 6. The aim of the experiments is to reduce the warming from that resulting from a high-tier emission scenario (Shared Socioeconomic Pathways SSP5-8.5) to that resulting from a medium-tier emission scenario (SSP2-4.5). These sim-
ulations aim to analyze the response of climate models to a reduction in incoming surface radiation as a means to reduce global surface temperatures, and they do so either by simulating a stratospheric sulfate aerosol layer or, in a more idealized way, through a uniform reduction in the solar constant in the model. We find that, over the last two decades of the century, there are considerable inter-model spreads in the needed injection amounts of sulfate (29 ± 9 Tg-SO_2/yr between 2081 and 2100), in the latitudinal distribution of the aerosol cloud, and in the stratospheric temperature changes resulting from the added aerosol layer. Even in the simpler G6solar experiment, there is a spread in the needed solar dimming to achieve the same global temperature target (1.91 ± 0.44 %). The analyzed models already show significant differences in the response to the increasing CO_2 concentrations for global mean temperatures and global mean precipitation ($2.05K \pm 0.42K$ and 2.28 ± 0.80 %, respectively, for SSP5-8.5 minus SSP2-4.5 averaged over 2081-2100). With aerosol injection, the differences in how the aerosols spread further change some of the underlying uncertainties, such as the global mean precipitation response ($-3.79 \pm$
0.76 % for G6sulfur compared to -2.07 ± 0.40 % for G6solar against SSP2-4.5 between 2081 and 2100). These differences in the behavior of the aerosols also result in a larger uncertainty in the regional surface temperature response among models in the case of the G6sulfur simulations, suggesting the need to devise various, more specific experiments to single out and

resolve particular sources of uncertainty. The spread in the modelled response suggests that a degree of caution is necessary when using these results for assessing specific impacts of geoengineering in various aspects of the Earth system. However, all models agree that, compared to a scenario with unmitigated warming, stratospheric aerosol geoengineering has the potential to both globally and locally reduce the increase in surface temperatures.

1   Introduction

Solar Radiation Modification (SRM) is defined as the proposed artificial altering of the radiative balance of the planet in order to temporarily counteract some of the imbalance produced by the increase in atmospheric greenhouse gases (GHGs). This might be achieved in multiple ways, but the most studied one, originally proposed by Budyko (1978) and Crutzen (2006) would consist of the injection of SO_2 into the stratosphere in order to produce a layer of sulfate aerosols capable of partially reflecting incoming solar radiation: this is usually defined as Stratospheric Aerosol Intervention (SAI), or Sulfate Geoengineering. Simulating such a technique in climate models is the main way of understanding possible impacts to the composition of the atmosphere and to the surface climate, to determine its eventual feasibility, understand its possible impacts on ecosystems and populations (Zarnetske et al. (2021)) and inform policymakers and stakeholders.

The Geoengineering Model Intercomparison Project (GeoMIP) has been proposed initially in Kravitz et al. (2011) as a way to standardize SRM modeling experiments, allowing for a more robust comparison between model responses and determine sources of uncertainties and areas for improvement. Whereas the term "geoengineering", "climate engineering" or, more recently, "climate intervention" [1] are usually used to consider also methods of Carbon Dioxide Removal (CDR), in the original intention of GeoMIP (and this work) it was only considered as a more colloquial term for SRM.

Two previous experiments in particular have been widely analyzed and discussed: G1, where the solar constant is reduced in order to offset the temperature increase produced by a 4×increase in CO_2 compared to pre-industrial concentrations (Kravitz et al. (2013b); Tilmes et al. (2013); Glienke et al. (2015); Russotto and Ackerman (2018b); Kravitz et al. (2020)) and G4, where a constant amount of SO_2 is injected into the equatorial stratosphere, under emissions from the Representative Concentration Pathway 4.5 (RCP4.5) (Pitari et al. (2014); Kashimura et al. (2017); Visioni et al. (2017b); Plazzotta et al. (2019). However, previously performed GeoMIP experiments were not intended to be "realistic" deployments of geoengineering, either because they were performed under idealized conditions (such as 4xCO$_2$ concentrations) or because they considered a fixed, constant amount of injected SO_2 with abrupt beginning and ending. In the case of the G4 experiment, furthermore, there was no scenario to compare in which similar global mean temperatures were achieved with lower CO_2 but no geoengineering. Two new experiments have been proposed as part of the GeoMIP Phase 6 (Kravitz et al. (2013b)) where geoengineering is aimed at lowering global mean surface temperatures from those in a high-tier emission scenario (Shared Socioeconomic Pathway - SSP5-8.5, Meinshausen et al. (2020)) to those in a medium-tier emission scenario (SSP2-4.5). G6sulfur aims to achieve this temperature goal by increasing the simulated stratospheric aerosol optical depth (AOD): in models with an interactive sulfur cycle and

---

[1]https://www.silverlining.ngo/us-national-survey-terminology-for-approaches-for-directly-influencing-climate

50   stratospheric aerosol microphysics, this is done by simulating the injection of SO_2 between 10°N and 10°S between 18 and 20 km, whereas in other models this is done by imposing a sulfate distribution calculated offline. G6solar, on the other hand, decreases total incoming solar irradiance. While the latter does not aim to reproduce the effects of an actual sulfate aerosol intervention, comparisons of its results with simulations of stratospheric aerosols in the same model may help understand the contributions to inter-model differences in the response to aerosols (Niemeier et al. (2013); Visioni et al. (2021)). Both reduc-

55   tions of incoming solar radiation at the surface (directly, by turning down the Sun, or indirectly, by having the aerosols reflect the solar radiation) are adjusted at least every decade to ensure that the target temperature is being met.

    There are multiple uncertainties that can be investigated with a multi-model intercomparison when considering the climate models' responses to an artificial, deliberate modification of surface temperatures by means of stratospheric aerosols (Kravitz

60   and MacMartin (2020)). In the stratosphere, these include the conversion of injected SO_2 into stratospheric aerosol and the subsequent large-scale distribution of the aerosols by the stratospheric circulation (not dissimilar to multi-model analyses of simulations of explosive volcanic eruptions, Marshall et al. (2018); Clyne et al. (2020)), the chemical response of key strato- spheric components (ozone, methane) to the aerosol layer (Pitari et al. (2014); Visioni et al. (2017b)), the magnitude of the produced local heating (Niemeier et al. (2020)), and the dynamical response. At the surface, uncertainties include the magni-

65   tude of the resulting global cooling per Tg-SO_2 injected or per unit of optical depth produced, the regional patterns of change in temperature (Kravitz et al. (2013a)), precipitation (Kravitz et al. (2013b); Tilmes et al. (2013)), and extreme events (Aswathy et al. (2015); Ji et al. (2018)) and other variables that might affect ecosystems and populations (Zarnetske et al. (2021)): for instance, tropospheric ozone (Xia et al. (2017)) or cloud changes (Russotto and Ackerman (2018a)).

70   In this work we analyze the response to the two proposed experiments in six global climate models, all part of the Climate Model Intercomparison Project, Phase 6 (CMIP6), in order to explore some of the described uncertainties in these state-of-the- art models. After briefly describing the participating models and the experimental set-ups, in Section 3.1, we first confirm that all models successfully manage to lower globally averaged surface temperatures from those of the underlying high emission scenario to those of the medium one. While in the case of a broad solar reduction there is no constraint on the maximum

75   achievable cooling, previous work has suggested a non-linear behavior between injected SO_2 and aerosol burden at high amounts of injections (Pierce et al. (2010); Niemeier and Timmreck (2015)), resulting in a reduced efficiency. Therefore we also try to evaluate the presence of a similar nonlinearity in the participating models (if it occurs in the range of forcing needed in our experiment). We then analyze in Section 3.2 differences in the latitudinal spread of the stratospheric aerosols cloud despite the consistent injection location. Even when pursuing the same global mean temperature-oriented goal, it has been

80   shown in simulations with CESM1(WACCM) that differences in the latitudinal (Kravitz et al. (2019) and seasonal (Visioni et al. (2020b)) distribution of the aerosols can result in significant differences in surface climate. If different models simulate different distributions of the aerosols (as it was for the G4 experiment, Pitari et al. (2014)) due to different stratospheric processes (both dynamical and chemical, Niemeier et al. (2020); Franke et al. (2020)), the simulated surface climate would also be different. Furthermore, even given similar simulated aerosol distribution, the stratospheric response might differ due to differences in

aerosol optics and in the radiative transfer calculation and in the representation of chemical processes in the stratosphere (i.e. if interactive chemistry is considered in the stratosphere, Franke et al. (2020)) resulting in a different dynamical and ultimately surface response (Simpson et al. (2019); Jiang et al. (2019); Banerjee et al. (2020)), which we discuss in Section 3.3 for annual mean temperature and precipitation.

2   Description of simulations

We analyze four sets of simulations from 2020 to 2100: two baseline scenarios without geoengineering that follow two Shared Socioeconomic Pathways, SSP2-4.5 and SSP5-8.5 (O'Neill et al. (2016)) and two scenarios with geoengineering, G6solar and G6sulfur (Kravitz et al. (2015)). Overall, six models participated in all experiments (Table 1).

In the SSP2-4.5 and SSP5-8.5, GHG emissions follow a medium and high trajectory respectively, resulting by the end of the century in a radiative forcing indicated by the last two numbers in the name (i.e., 4.5 and 8.5 W/m^2, similar to the Representative Concentration Pathways in CMIP5). The G6 simulations start in 2020 with the same emissions as SSP5-8.5 and, on top of that, have either the solar constant reduced by a certain fraction or produce a sulfate aerosol optical depth with the aim of reducing the globally averaged surface temperature down to the SSP2-4.5 level. While the solar reduction is performed in the same way in all G6solar experiments, reducing the solar constant uniformly at all latitudes, not all participating models included stratospheric aerosols by directly injecting SO$_2$. Two models (IPSL-CM6A-LR and UKESM1-0-LL) injected SO$_2$ uniformly between 10°N and 10°S between 18 and 20 km of altitude and across a single longitudinal band (°0). CESM2(WACCM) injected SO$_2$ at the Equator and at 25 km of altitude. The others prescribed an already-calculated aerosol optical depth distribution: CNRM-ESM2-1 used an input dataset provided by GeoMIP (the aerosol distribution the G4SSA experiment Tilmes et al. (2015)), while MPI-ESM prescribed their own aerosol distribution derived from the simulations described in Niemeier and Schmidt (2017) and Niemeier et al. (2020). In both cases, the prescribed aerosols are fully integrated in the radiative transfer calculations. Therefore, the response of direct and diffuse radiation at the surface and the localized stratospheric warming due to radiative heating are fully consistent with those from the other models where the full aerosol production from SO$_2$ is simulated (see for instance Laakso et al. (2020)). However, previous studies have shown the presence of non-linearities at higher injection loads. These can be microphysical in nature, with aerosol particles growing to larger sizes with larger loads of SO$_2$ (Niemeier and Timmreck (2015)) or dynamical, with the stratospheric heating producing changes in stratospheric circulation resulting in a different aerosol distribution in the tropics (Visioni et al. (2018b)) or at high-latitudes (Visioni et al. (2020a)). If the same aerosol distribution is simply scaled up, these effect would not be present in those models.

A summary of models participating, ensemble size, and notes related to the implementation of G6sulfur is provided in Table 1. Further information on the models' components can be found in the references provided for each model, and a summary is given in Table S1. More detailed information for CMIP6 models can also be found in Séférian et al. (2020) for marine biogeochemistry, Arora et al. (2020) for carbon-climate feedbacks and Thornhill et al. (2021) for atmospheric chemistry.
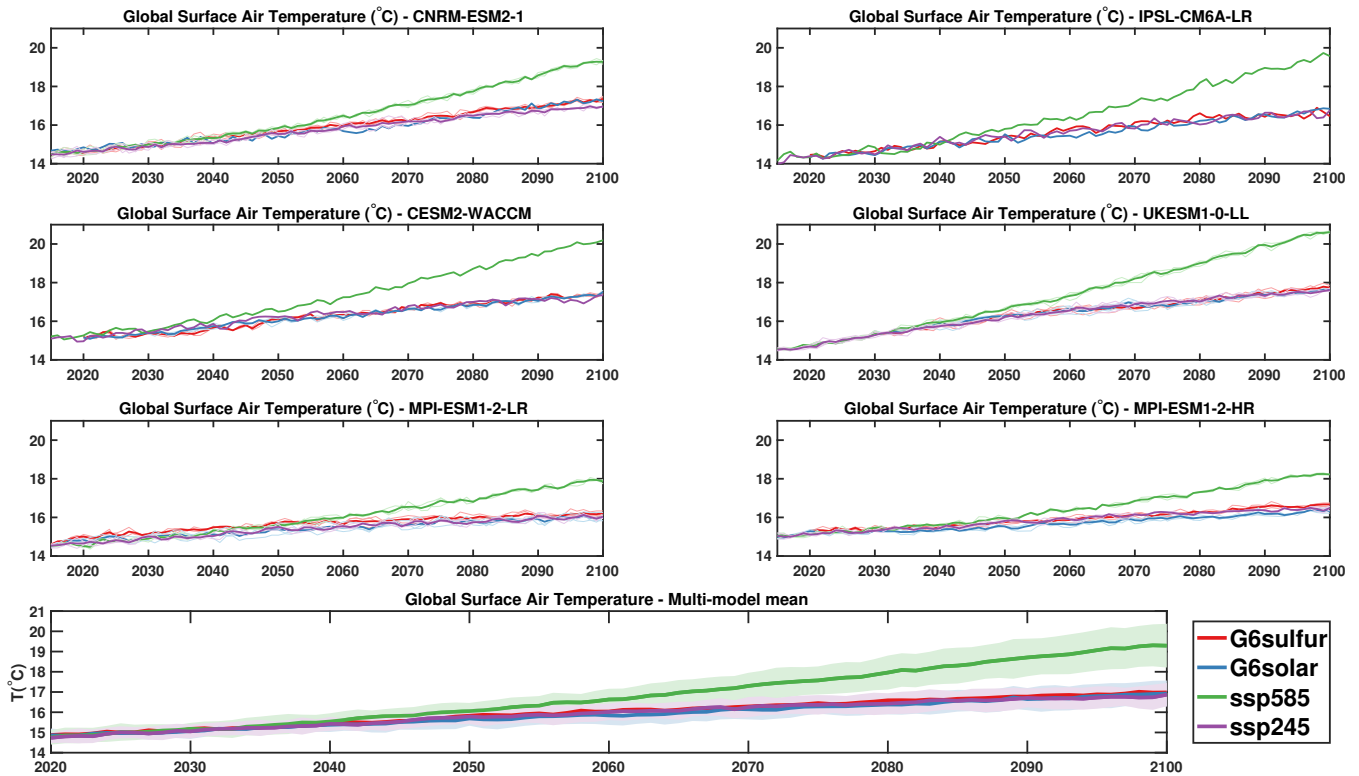
Figure 1. Global mean surface temperatures ($^{\circ}$C) for the four experiments for each participating model. Single ensemble realizations are shown in lighter lines, while the ensemble mean is shown in thicker lines. The multi-models mean is shown at the bottom, with the shading representing 1σ standard deviation of the mean for each experiment.

Two modeling teams, IPSL-CM6A-LR and UKESM1-0-LL, determined every decade how much to reduce the solar constant by or how much more SO_2 or prescribed aerosols to have in the stratosphere in order to reduce surface temperatures of the forthcoming decade to SSP2-4.5 levels, whereas four, CESM2(WACCM), MPI-ESM1.2-LR, MPI-ESM1.2-HR and CNRM-ESM2-1, did so every year. For CESM2(WACCM), the determination of injected SO_2 or reduction of the solar constant is done by a feedback algorithm described in Kravitz et al. (2017) and also used in Tilmes et al. (2018a, 2020).

3 Results

3.1 Magnitude of geoengineering required

All models successfully reduce global-mean surface air temperatures to SSP2-4.5 levels to within 0.2°C of SSP2-4.5 levels on average throughout the century with both geoengineering methods (Fig. 1), but the amount of geoengineering required to do so varies across models. There are a variety of overlapping mechanisms that contribute to these differences. As reported in Table 2, the models produce a large spread in the projected warming produced by the two scenarios. Similar inter-model

spreads have been reported in the recent literature for CMIP6 models for both effective Equilibrium Climate Sensitivity (ECS, the equilibrium warming for a doubling of CO_2, see Zelinka et al. (2020)) and Transient Climate Response (TCR, the temperature warming with a doubling of CO_2 in a scenario with a 1% per year CO_2 increase, see Meehl et al. (2020)). Some models (amongst them CESM2(WACCM) and UKESM1-0-LL, present in this study also) have been found to have values well above previously established likely ranges for both ECS and TCR (Gettelman et al. (2019); Sherwood et al. (2020)). Some of the relationships between the variables reported in Table 2 are explored in Fig. 2: a weak relationship between the different warming in the SSP scenarios and ECS and TCR is to be expected due to differences in both the timescale of the response and the differences in, for instance, other GHGs and tropospheric aerosols (Hansen et al. (2005)) that affect the climate in the short period and that are not factored in the long-term response to CO_2 changes. For instance, CNRM-ESM2-1 reported an ECS of 4.79 K (Zelinka et al. (2020)) (the second highest here) but a ΔT of 1.9 K (the third lowest).

This implies that even if different models agreed on how much either stratospheric AOD or reduction in the solar constant would be needed to cool globally by 1K (the efficacy of the geoengineering method), the overall reported amount of intervention needed would be different due to the different response to the forcing from CO_2. To first order, there should be no expectation that the sensitivity of climate models to a CO_2 increase should be related to the reduction in temperature due to geoengineering (Kravitz et al. (2020)), and we indeed show this in Fig. 2. In Fig. 2f we show that normalizing the required solar dimming or produced AOD in the last two decades to the global cooling in the same period slightly increases the inter-model spread, from 19.9 % to 22.8 % for solar dimming and from 17.2 % to 20.7 % for AOD compared to the mean (the same quantities, not normalized, are shown in Fig. S1). In Fig. 2e we also show that the amount of solar reduction and the globally averaged stratospheric AOD seem to be only weakly related (R^2=0.72), suggesting that there are different mechanisms involved in the cooling due to the aerosols and the cooling due to reduced insolation. For G6sulfur, this might be due not only to the radiative treatment of the aerosols themselves, but also to different latitudinal distribution in AOD resulting in different forcing, compared to the broad solar reduction that is nearly spatially identical in all models.

The time-dependent amount of geoengineering needed in all models for the two experiments is reported in Fig. 3a-b, together with the top-of-atmosphere (TOA) forcing imbalance between SSP5-8.5 and SSP2-4.5, calculated as the incoming minus the outgoing longwave and shortwave radiation (Fig. 3c), and the underlying difference in CO_2 concentration, common to all models, as prescribed for the SSP scenarios in Meinshausen et al. (2020) (Fig. 3d). In terms of TOA forcing, models show a more consistent forcing that is a result, mostly, of the same CO_2 increase, but then they disagree both in the magnitude of the warming produced by this same forcing (as shown in Fig. 1) and in the amount of intervention (optical depth, or solar reduction) needed to overcome that forcing, as shown in panels 3a and 3b. The comparison between the two forcings is also useful to understand the behavior of the geoengineering amount in the models in the first 30 years, where most models indicate little to no geoengineering is necessary. CESM2-WACCM is an exception, and indeed shows a slight overcooling in the first decades compared to other models: this is most likely a feature of the current feedback controller, as has been observed in Tilmes et al. (2018a): the algorithm, which decides how much to inject each year by learning from past years, requires some
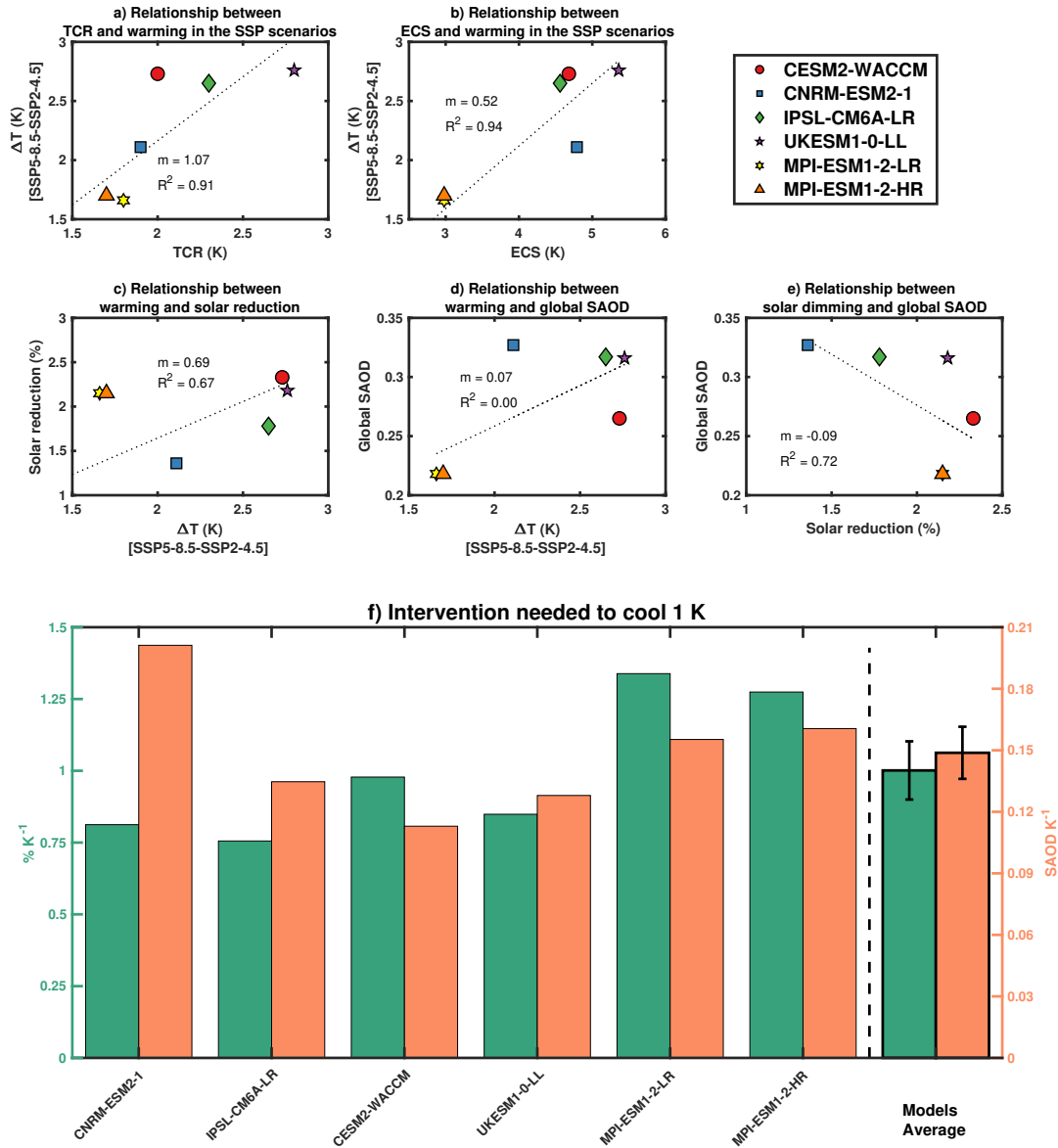
Figure 2. Panels a-e): scatter plot of various relationships between some global quantities in the participating models. ΔT between SSP5-8.5 and SSP2-4.5, global stratospheric aerosol optical depth (SAOD) and solar reduction are defined in the 2081-2100 period. Transient Climate Response (TCR) and effective Equilibrium Climate Sensitivity (ECS) are taken from Zelinka et al. (2020) and Meehl et al. (2020). The R^2 and the slope of the linear fit (m) are shown for each panel. f) Values in panel c-d) normalized by the ΔT in the same model, to obtain the normalized intervention (green for solar dimming and orange for stratospheric AOD) needed to cool by 1K, with multi-model average on the right and error bars indicating the standard error

time to properly converge before it can successfully determine the necessary amount. More generally, the small differences between the two underlying scenarios in terms of global mean temperature in the first three decades tend to magnify small differences in the required intervention, as manually estimated by the modeling teams, resulting in larger differences in the first years. Later in the century, when the temperature difference is larger and the intervention scales up, inter-model differences may be explained by the presence of non-linearities or other effects (such as an increase in stratospheric water vapor, Visioni et al. (2017a)). It is interesting to note that, while a large portion of the models do not vary the amount of geoengineering smoothly, but once a decade, the applied step-function is not evident in the globally averaged surface temperature responses shown in Fig. 1, where there is no qualitative difference between models in terms of decadal variability: since it is similarly present in the G6solar experiments, the reason for this may be found in the slower oceanic response. Future analyses should investigate whether the step-function introduced by some of the models results in changes in surface climate that, while hidden when considering global or decadal averages, might be present when looking at particular regions or climate features (for instance, the monsoon season) in the years where the step change is present.

3.2 Differences in the stratospheric response

For the G6sulfur simulations, the global mean AOD is not, on its own, enough to understand different models' behavior. Different spatial distributions of the aerosol layer, while yielding similar global values, might result in different efficiency and would produce different responses of the surface climate (MacMartin et al. (2017); Kravitz et al. (2019); Visioni et al. (2020b)). Reasons for a different aerosol distribution with similar injection locations and height of SO_2 can be the different dynamical features of the simulated stratosphere and/or differences in the aerosol microphysics schemes (Pitari et al. (2014); Niemeier et al. (2020); Franke et al. (2020)) resulting in different aerosol growth, transport and sedimentation, as already shown for simulations of explosive volcanic eruptions (Marshall et al. (2018); Clyne et al. (2020)). The response to the presence of the aerosols themselves can in turn produce differences in stratospheric dynamics, for instance interacting with the Quasi-Biennial Oscillation (Aquila et al. (2014); Richter et al. (2017)), strengthening the tropical confinement of the aerosols (Niemeier and Schmidt (2017); Visioni et al. (2018b)).

Furthermore, even given similar annually-averaged AOD distributions, differences in the seasonal cycle might lead to different surface climate (Visioni et al. (2020b)). The spatial distributions of AOD for the last decade of the experiment in each model are shown in Fig. 4a. Results vary widely between models: UKESM1-0-LL represents a clear outlier in the tropics, with more than twice the sulfate AOD as other models. At high latitudes, on the other hand, there is a much larger inter-model spread, with values ranging from 0.1 to 0.3 at 90°S and from from 0.2 to 0.45 at 90°N. Strong disagreement between model-simulated AOD in a geoengineering scenario was already reported in Pitari et al. (2014) and Plazzotta et al. (2018) for the G4 experiments, where a 5 Tg-SO_2/yr injection in the equatorial stratosphere was prescribed in the simulation protocols. No models used in that experiment have been used in the G6 scenarios, so a direct comparison can't be done with different versions of the same models. In this case, however, we can note that all models at least agree on the presence of a confinement of a portion of the aerosols in the tropical pipe, whereas in G4 half of the models reported much less AOD in the tropics and more at very
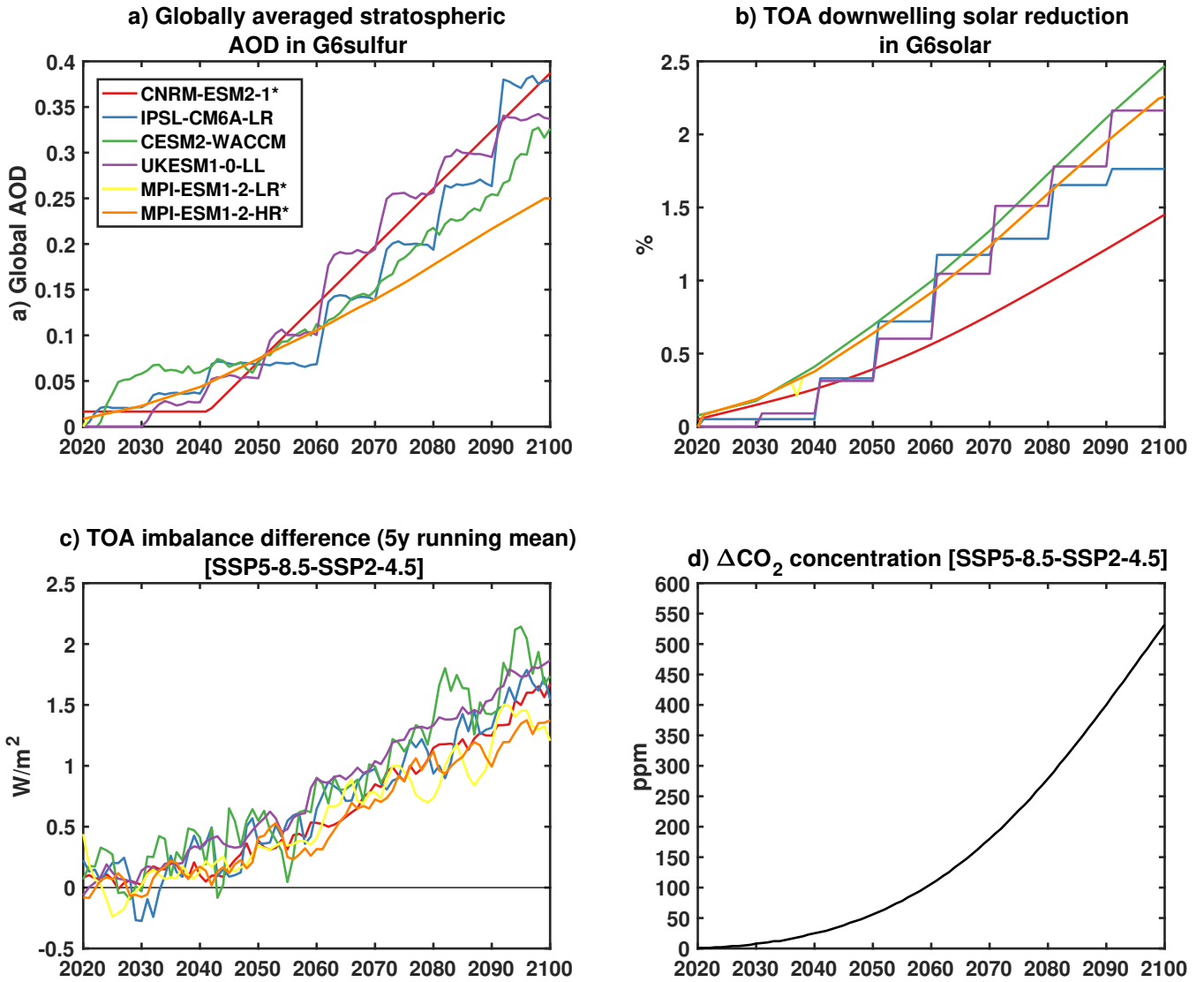
Figure 3. Time-dependent evolution for all participating models of: a) globally averaged stratospheric AOD increase in the G6sulfur experiment (models with an asterisk in the legend have prescribed AOD. The orange and yellow line for the two MPI-ESM1-2 versions completely overlap); b) solar reduction in the G6solar experiment as a fraction of the overall incoming solar radiation; c) Top-of-atmosphere radiative forcing imbalance (downwelling solar radiation minus upwelling solar+longwave radiation) difference between the two baseline SSP scenarios; d) difference in CO_2 concentration between the two emission scenarios from Meinshausen et al. (2020) presented for reference.

high latitudes (Pitari et al. (2014)), which is physically very unlikely given observations from the Pinatubo eruption in 1991 (Robock (2000); Pitari et al. (2016)).

200   Model spread on a particular result is not, of course, the same as uncertainty: models may agree despite a lack of observational support, resulting in a narrow spread that might be inaccurate, or the spread might be large because some model results are simply inconsistent with available observations. Here we try to better constrain the distribution of AOD in the various models in G6sulfur using the up-to-date CMIP6 dataset for volcanic forcing, that combines measurements from various sources (Dhomse et al. (2020), retrieved from ftp://iacftp.ethz.ch/pub_read/luo/CMIP6/, last access: October 29, 2020). In particular,

205   using the 550 nm extinction data, we derive the stratosphere-only latitudinal distribution of the optical depth following the Pinatubo 1991 eruption, averaged from 1 month after the eruption (July 1991) to 1 year after, in order to also consider the poleward transport of the aerosols. It needs to be highlighted that the comparison between an impulsive injection (as Pinatubo) versus a sustained injection (as in the geoengineering experiment) is an imperfect one, both in terms of the aerosol distribution and in terms of the effects on surface climate (Duan et al. (2019)), but it is possibly the only "real", albeit imperfect, point of

210   comparison between model behavior and the actual atmospheric behavior. In the case of a volcanic eruption, the precise meteorological conditions strongly influence the resulting AOD; furthermore, the SO_2 is injected in a clean stratosphere. Therefore, the following comparison should not be considered as a way of measuring which model is closer to observations, but just as a way to compare the different models when they reach a similar global AOD. In Fig. 4c we report the AOD from Pinatubo derived this way, and we then compare the results with those from the various G6sulfur models. To do so, we consider the year

215   in which each model reaches the same global value of AOD as Pinatubo, and plot the latitudinal distribution of AOD for each model in that year. This comparison highlights various elements that would be lost considering the results towards the end of the century as in Fig. 4a: models show a higher agreement considering a moderate level of global AOD reached, and compared with the results from Pinatubo (considering the differences in meteorology and injection location) they look reasonable. In particular, UKESM1-0-LL and CESM2-WACCM show a better agreement in their tropical AOD, as opposed to what was

220   shown in Fig.4a, indicating the presence of non-linearities at high injection rates, that might be induced in UKESM1-0-LL by a too strong confinement of the aerosols in the tropical pipe as a consequence of the dynamic response to heating (Aquila et al. (2014); Niemeier and Schmidt (2017); Visioni et al. (2018b). In Fig. 4c models show a much better agreement also at high latitudes (at least in the northern hemisphere) compared to Fig. 4a, with the exception of the prescribed AOD in CNRM-ESM2-1. This suggests that when considering higher injection loads, there could be a stronger interaction of the produced dynamical

225   changes with the simulated AOD at high latitudes (Visioni et al. (2020a)).

The amount of SO_2 needed to reach a certain stratospheric AOD varies considerably between climate models with interactive stratospheric aerosols even for simulations of Pinatubo, ranging in current estimates between 10 and 20 Tg-SO_2 with a central value of 14 (Timmreck et al. (2018)). In the G6sulfur experiments, the models show discrepancies in the estimate of the

230   amount needed to achieve a similar global AOD as in Pinatubo (with a multi-model average of 9.3 $\pm$ 2.3 Tg-SO_2, see table in Fig. 4) , closer to the lower limit from Timmreck et al. (2018) (10 Tg-SO_2) for UKESM1-0-LL and IPSL-CM6A-LR and 60%

lower for CESM2-WACCM. For CESM2-WACCM, the difference could be partially explained by the difference in altitude for the SO_2 injections. In Fig.4c we also report the cooling produced by the G6sulfur aerosols, compared to SSP5-8.5 in the considered year (we used a 5-years average around that year to reduce the contribution of natural variablity). For Pinatubo, there is uncertainty in the cooling produced by the volcanic aerosols due to the precise meteorology of that year (for instance, the influence of an El-Niño event or other climatic oscillations compared to the years immediately before/after): Parker et al. (1996) estimate a global cooling of around 0.4 K, and similarly Soden et al. (2002) estimated a range between 0.3 and 0.5 K, whereas more recent estimates by Canty et al. (2013) found a cooling of 0.14 K when considering the Atlantic Multidecadal Variability. The multi-model average for the G6sulfur simulation is very similar to the higher estimates, at $0.46K \pm 0.09$, but there is a large range in the single values from 0.24 (in MPI-ESM1-2-LR) to 0.74 (for CESM2-WACCM). The two global coolings could be hard to compare, however, due to their different nature (impulsive versus sustained). Overall, the comparisons shown in Fig. 4 raise an important point that should be taken into account when analysing G6 simulations in future works: while limiting the analyses towards the end of the century might yield a higher signal-to-noise ratio, it also risks magnifying uncertainties related to non-linear processes in the stratosphere. In Fig. S2, we also report the yearly evolution of the latitudinal distribution of AOD for models that inject SO_2, normalized by the amount of SO_2 injected in that year, which clearly shows the decrease in efficiency at higher injection loads.

As mentioned before, the presence of the aerosols in the stratosphere also produces a perturbation of stratospheric dynamics (Richter et al. (2017); Visioni et al. (2020a)) that, in turn, might affect precipitation (Simpson et al. (2019)) and temperature (Jiang et al. (2019)) at the surface. The response is driven by the absorption of infrared radiation by the aerosols resulting in the heating of the stratospheric air, and is thus dependent on the overall burden and the size of the particles (Pitari et al. (2016)), but also on interactions with the chemical cycles in the stratosphere (Visioni et al. (2017b); Richter et al. (2017)) and the incursion of water vapor from the troposphere due to the warming of the tropopause layer (Visioni et al. (2017b); Tilmes et al. (2018b); Boucher et al. (2017)). In Fig. 5 we show the stratospheric temperatures in the last decade of the G6sulfur experiment for all models. Interestingly, the model with the highest AOD in the tropics, UKESM1-0-LL, is also one of the models showing the least amount of stratospheric heating, whereas IPSL-CM6A-LR, with an average tropical AOD (but much larger SO_2 injection needed to achieve it) shows a temperature change that is much larger than others. The reasons for this may depend on multiple aspects that would need to investigated separately: for instance these might be a different size distribution of the stratospheric aerosols or a different concentration of particles (shown in Fig. 5) differences in ozone changes resulting in different heating rates (Richter et al. (2017); Niemeier et al. (2020), heating from stratospheric water vapor (Pitari et al. (2014); Simpson et al. (2019) or differences in the radiative schemes between models.

3.3 Surface climate response

When geoengineering the climate, reducing incoming solar radiation (either simulating stratospheric aerosols, or by reducing the solar constant in models) to obtain the same global surface temperature as a scenario with lower GHGs does not assure that regional temperatures follow the same pattern. This has been reported in climate model simulations of various complexity,

d) Year with the same AOD as Pinatubo

Model	Year	Tg-SO$_2$	dT
CNRM-ESM2-1	2056	N/A	0.27
IPSL-CM6A-LR	2062	10.0	0.55
CESM2-WACCM	2058	6.2	0.74
UKESM-1-0-LL	2054	9.4	0.50
MPI-ESM1-2-LR	2060	11.6	0.24
MPI-ESM1-2-HR	2060	11.6	0.24
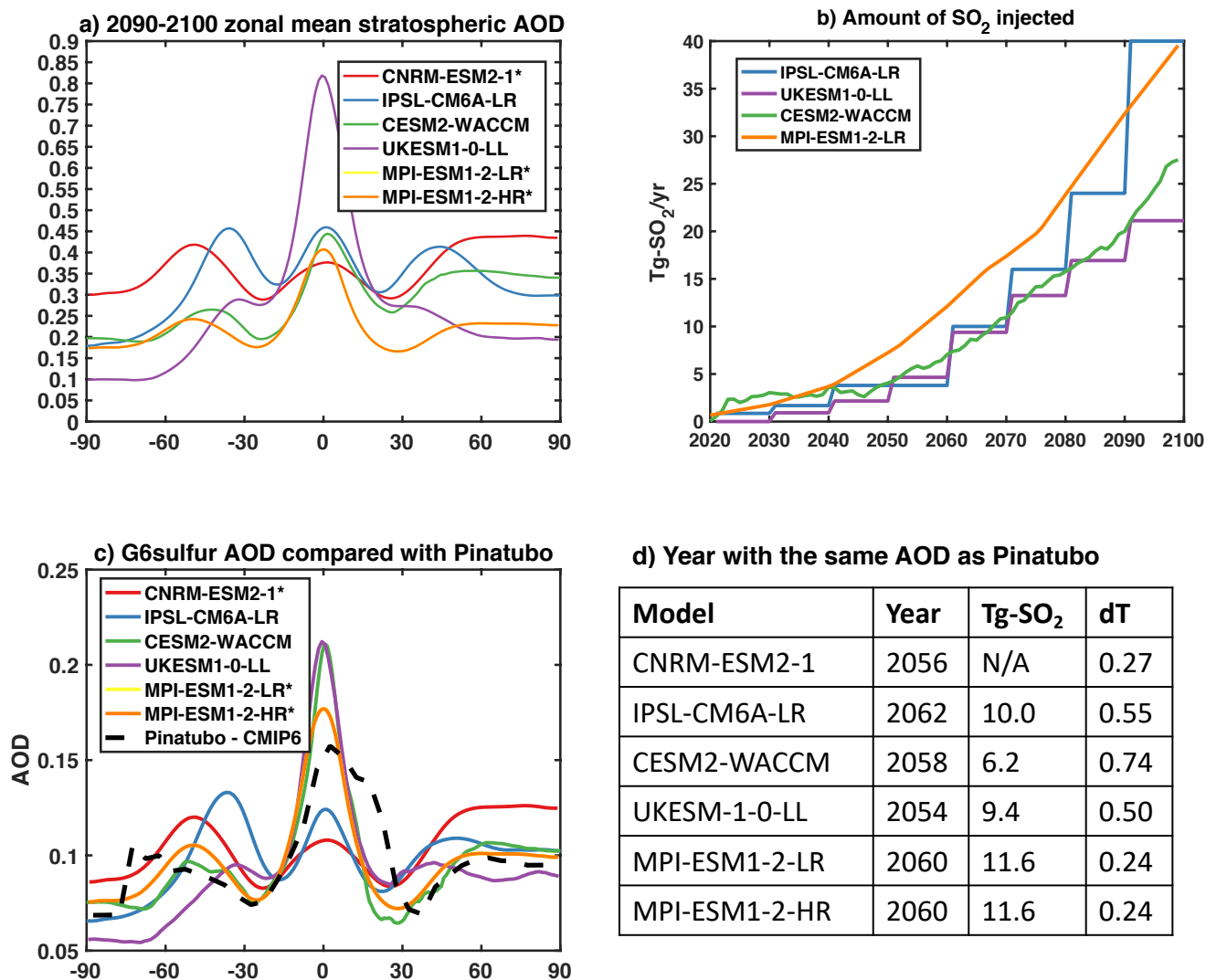
Figure 4. a) Stratospheric AOD in the last decade of the experiment for all participating models. The asterisk in the legend indicates models with prescribed optical depth. b) Injected SO$_2$ for available models, in Tg-SO$_2$/yr. c) AOD distribution for each model in the year with a global AOD closest to that from Pinatubo (0.102, averaged from July 1991 to June 1992), and comparison with the latitudinal distribution for the volcanic eruption following the new CMIP6 composed dataset (Dhomse et al. (2020)). In the box d), the year where the global value of AOD reaches 0.102 in the model is indicated, together with the amount of SO$_2$ needed to achieve that value and the cooling produced in G6sulfur compared to SSP5-8.5 in that year. Models marked with an asterisk in the legend used prescribed aerosol distributions for G6sulfur. The orange and yellow line for the two MPI-ESM1-2 versions always overlap.
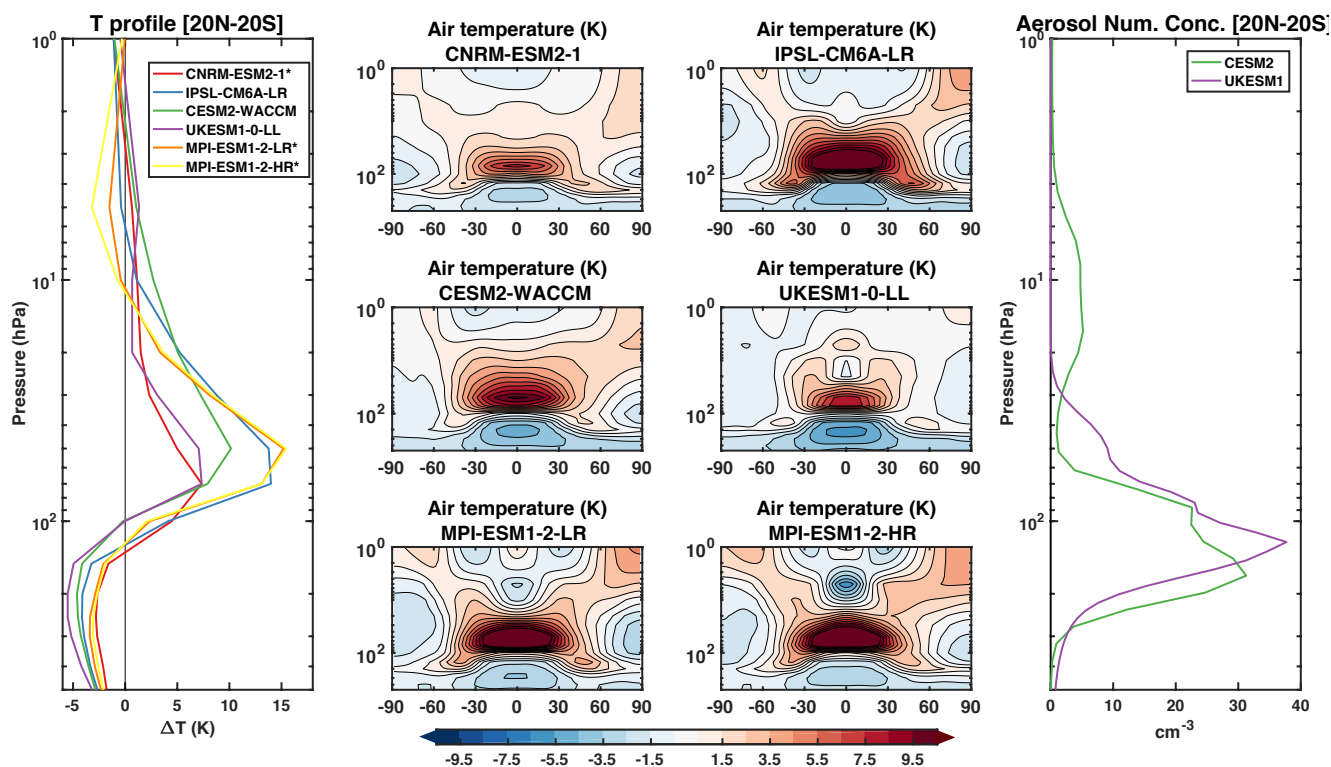
Figure 5. Profile of stratospheric temperatures changes (G6sulfur minus SSP5-8.5) between 20°N and 20°S are shown in the left panel. In the central panels, the changes are shown for each participating model. Profile of aerosol number concentration are shown in the right panel for a select number of models where output was available. All changes are for the years 2081-2100, and evaluated against the same period for the underlying emission scenario SSP5-8.5)

from 1-D models (Henry and Merlis (2020)) to Earth System Model simulations (i.e., Ban-Weiss and Caldeira (2010); Niemeier et al. (2013); Jones et al. (2018); Visioni et al. (2021)). These differences may be reduced if, together with reducing global temperatures, the geoengineering strategy aims to also reduce differences in higher-order temperature gradients (Kravitz et al. (2016); Tilmes et al. (2018a), but they cannot be completely cancelled due to various factors. First and foremost, a fundamental

270 difference in the radiative perturbation from CO_2 (that warm throughout the atmospheric column) and from the reduction in solar constant (that cool from the bottom-up) (Ban-Weiss and Caldeira (2010); Henry and Merlis (2020)) and from their seasonal and latitudinal differences (Govindasamy et al. (2003); Ban-Weiss and Caldeira (2010); Visioni et al. (2020b)) and surface climate effects (such as precipitation changes) of the stratospheric heating produced by the aerosols (Simpson et al. (2019); Visioni et al. (2021); Jones et al. (2021)). Other factors may also be an inability to restore the same state for the ocean

275 circulation: this latter point has been observed for instance in CESM1(WACCM) in Fasullo et al. (2018), and in one of the models that performed G6 simulations, CESM2(WACCM) in Tilmes et al. (2020).

All of these differences are compounded with those already present in climate models for regional temperature projections for CO_2 increases: on this point, however, MacMartin et al. (2015) argued that reducing surface temperatures through geo-engineering has the potential to actually reduce model spread in regional projections. That work however considered the G1 experiment, that entails a uniform solar reduction to reduce temperatures under a $4\times CO_2$ increase. Clearly then, most of the differences listed above are not included in such an idealized experiment. This is clear when looking at the multi-model averages of surface temperature differences shown in Fig.6: the simulated differences with SSP2-4.5 are much larger in G6sulfur compared to G6solar, and also the inter-model spread is much larger in G6sulfur. This indicates that there is better agreement between models when the uncertainties related to the stratospheric sulfate are removed. For G6sulfur, there is a general agreement in the inability of sulfate geoengineering to completely cool down the northern high-latitudes, partly due to the focus of the geoengineering strategy on reducing global mean temperatures (Kravitz et al. (2019)), but also probably due to the presence of stratospheric heating (Jiang et al. (2019)), as evident by the absence of high-latitude warming with the same magnitude in the G6solar simulations. The residual warming present also in the G6solar simulations can be partly explained by the differences in the radiative forcing from the CO_2 and the solar reduction (Ban-Weiss and Caldeira (2010); Henry and Merlis (2020); Visioni et al. (2021)). Differences in the surface response between models would thus depend on how different models physically reproduce some of the processes mentioned, but also on the differences in the stratospheric response reported in the previous section: different latitudinal and seasonal distributions of the aerosols produce different climate states even just in the same model (as shown in CESM1(WACCM) in Kravitz et al. (2019); Visioni et al. (2020b)), and the stratospheric heating is also reportedly different as shown in Fig. 5. Nonetheless, the essential finding from MacMartin et al. (2015) still holds when comparing the multi-model standard error for the geoengineering projections against those for the SSP5-8.5 changes, that especially over land and at high latitudes are always higher than both G6 cases.

We report the surface temperature maps for the last two decades of the experiment for each model in Fig. 7, from which some observations can be made that would not be immediately evident from the multi-model average. For G6sulfur, there is a good agreement regarding the residual warming over Northern Eurasia across models, with the exception of CESM2. There is less agreement over North America, where some models simulate a cooling in G6sulfur compared to SSP2-4.5 while some simulate a warming. This might be due to differences in the response of the North Atlantic circulation both to increasing GHGs and to geoengineering (Tilmes et al. (2018a, 2020)). Comparing this result to that from G6solar, where there is a concurrence of all models in simulating a small warming over the same region, might indicate that the much different response in G6sulfur might on the other hand be due to differences in the distribution of the stratospheric aerosols: UKESM1-0-LL, for instance, where more residual warming is present, shows the lowest AOD over high latitudes (Fig. 4). In the tropics, in the Amazon region models seem to differ more in the G6sulfur case and less in the G6solar case: possible causes might be an influence from the different magnitude of AOD in that region, different responses of the vegetation to increasing CO_2 concentrations and reduced solar radiation (Simpson et al. (2019)) or local changes in atmospheric circulation (Jones et al. (2018)).
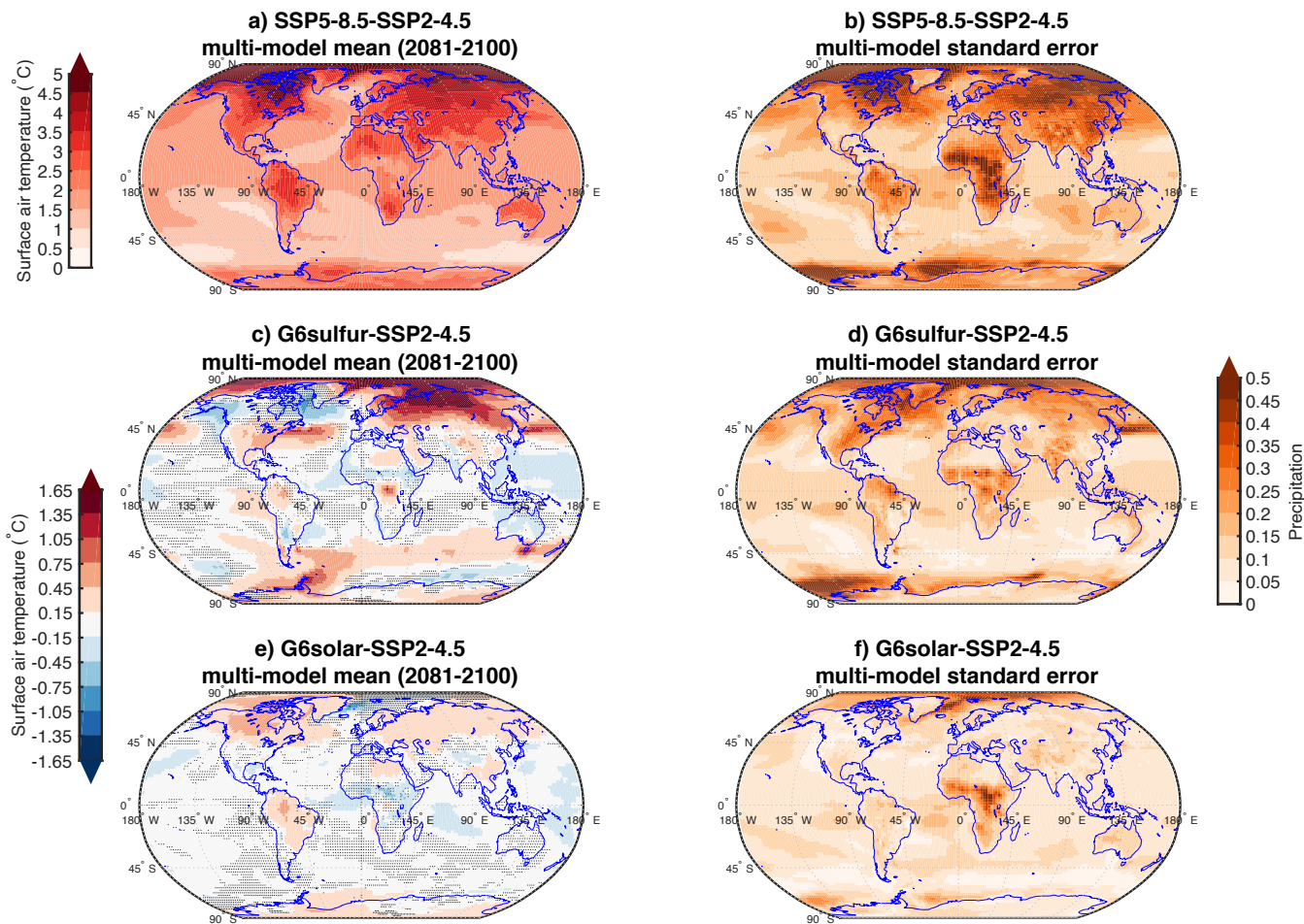
Figure 6. Left column: multi-model averages for surface temperatures changes averaged over 2081-2100 in different cases (a) SSP5-8.5; c) G6sulfur; e) G6solar) minus the same period for SSP2-4.5. Etched areas (in grey) indicate where less than 66% of models (here, 4 out of 6) agree on the sign of the difference in that grid-point. Note the different colorbar between panel a) and panels c-e). Right column: Standard error in the multi-model mean for the same reference case on the left. All models results have been re-gridded using a common grid equivalent to that from the model with the lowest horizontal resolution.

Overall, the inter-model differences indicate the need for some care when trying to understand the possible surface impacts of sulfate geoengineering by using multi-model ensembles. It might be difficult to correctly separate the differences in surface impacts due to differences in the stratospheric AOD (shown in Fig.4) given a similar injection, and those produced by different response of the surface climate. While comparing results with those from a similar, more uniform experimental design such as

315 G6solar might help, the lack of the potential response produced by the aerosols (Banerjee et al. (2020); Visioni et al. (2021)) may suggest the use of a prescribed aerosol distribution for various models (Tilmes et al. (2015)) as an intermediate approach. This can also be seen in the comparison between the two version of MPI (that differ only in their horizontal resolution, which is twice as high in the HR version): they both use the same AOD distribution, and have the same magnitude of stratospheric AOD in the whole period. Yet, they show some considerable differences in the surface temperature response to the same aerosol (or

320 even solar) forcing. In particular, the warming observed over North America in the LR version is not as high in the HR version, whereas the warming present in West Antarctica in the HR version is not present in the LR version. This might indicate that regionally the temperature response may be due to different response of the deep ocean circulation (in the West Antarctica case) as also shown in McCusker et al. (2015), and that this might be model dependant (other than depending on the particular injection strategy); or to a different response of the atmospheric circulation (Jones et al. (2018)). On the other hand parts of

325 the response, such as the patches of warming present in the Amazon and in Central Africa, possibly due to a different land response, are shared between the two versions, and similarly a large part of the warming over Eurasia. While observing the response of different versions of the same model to the same forcing might point to some of the causes, comparing that to the response of a different model to the same forcing may also highlight which parts of the overall response is model-dependant, and which is robust across models.

330 Surface temperatures are not the only measure of the possible impacts of either climate change or geoengineering: amongst the many others, hydrological cycle changes are also central to any assessment. Under climate change, due to the surface and tropospheric warming allowing for more moisture to be retained by the air, global precipitation has been consistently projected to increase (Pendergrass and Hartmann (2014)), and a similar behavior is displayed by the models participating in the G6 experiments (8). Similarly, it has been widely assessed that trying to restore surface temperature to a previous state by

335 means of modifying the top of the atmosphere radiative balance tends to overcompensate the changes in precipitation, therefore reducing global mean precipitation. Globally, the changes are driven by the perturbation of the surface heat fluxes (Tilmes et al. (2013); Kravitz et al. (2013b); Niemeier et al. (2013)) and changes in sea-land temperature contrast: regionally however, the modification of the baseline distribution of precipitation can be due to changes in the Inter-tropical Convergence Zone (ITCZ, Russotto and Ackerman (2018b); Cheng et al. (2019)) produced by changes in the inter-hemispheric temperature gradient,

340 general circulation changes produced by stratospheric heating (Simpson et al. (2019)) and regional and seasonal changes in heat fluxes and temperature gradients (Jones et al. (2018); Visioni et al. (2020b)). In the case of sulfate injections, these changes can be strongly dependent on latitudinal and temporal distribution of the aerosol cloud as well (Kravitz et al. (2019); Visioni et al. (2020b)).

The response of the various models for the G6 experiments in Fig. 8 is in agreement that the global-mean precipitation would

345 be overcompensated (Niemeier et al. (2013)). However, models disagree on the magnitude of this overcompensation, and in
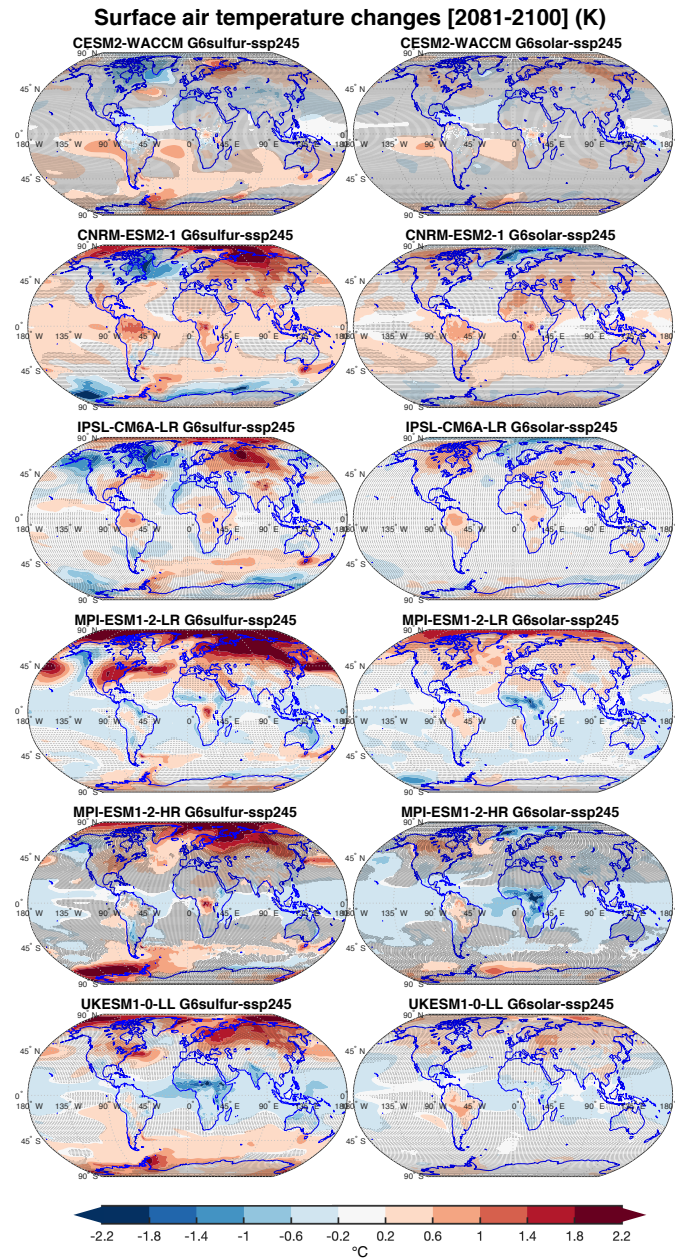
Figure 7. Surface temperatures changes in the period 2081-2100 in G6sulfur compared to the same period for SSP2-4.5 in G6sulfur simulations (left panels) and G6solar simulations (right panels) for all participating models. Shaded areas indicate where the difference is not statistically significant, evaluated using a double-sided t-test with p<0.05 on the ensemble averages for each model, considering all 20 years as independent samples.

the difference between G6solar and G6sulfur. The fact that under the SSP2-4.5 scenario some warming continues during the 21st century, combined with the precipitation overcompensation by geoengineering, results in some models in no changes in global precipitation compared to the beginning of the century (as already noted in Irvine and Keith (2020)): only G6sulfur in IPSL-CM6A-LR shows a decrease compared to that period by the end of the century. For the purpose of future analyses, the anomalous global precipitation response in the MPI models for G6sulfur has to be noted: it is very likely that the slightly larger response in global mean precipitation at the beginning of the century is due to differences in the initialization process for those simulations, rather than in a change produced by the sulfate (which is very close to zero, in 2020), and results before 2050 (for the LR version) or 2040 (for the HR version) should not be considered as representative.

From the prospect of assessing ecosystem impacts, this decoupling of precipitation, temperatures and CO_2 should be investigated in depth to understand if and where it would be beneficial or not. It also further stresses the notion that reducing precipitation is not an automatic result of geoengineering, but that the outcome is related to which specific cooling targets geoengineering is deployed to achieve (Tilmes et al. (2013); Irvine et al. (2019); Lee et al. (2020)). All models agree, to various degrees, that global precipitation changes under G6sulfur are larger than the same changes under G6solar: there might be various reasons for this, such as differences in latent heat due to different ratios of diffuse solar radiation (that increases in the case of the sulfate aerosols, Visioni et al. (2021)) resulting in more atmospheric absorption, changes in cloud formation produced by the different vertical atmospheric temperature gradient. Niemeier et al. (2013) suggested that the reason for this might be found in the stratospheric heating produced by the aerosols resulting in more water vapor entering the stratosphere from the warming of the tropopause layer (Tilmes et al. (2018a); Simpson et al. (2019)) producing a small positive radiative forcing whose warming effect (Hansen et al. (2005); Visioni et al. (2017a)) needs to be counterbalanced by injecting slightly more aerosols.

Lastly, models agree on regional precipitation changes more in G6solar than in G6sulfur (Fig. 9), but all models project most of the significant changes will occur over the tropics (where also most of the baseline precipitation is located), but with some significant local differences between models (Fig. 10): for instance, while CESM2-WACCM shows less precipitation in the tropical northern hemisphere and more precipitation in the tropical southern hemisphere, UKESM1-0-LL presents a drying in both hemispheres, especially over continents. In some cases, such as at high northern latitudes, all models show a positive change in G6sulfur, and a negative change in G6solar. It is again interesting to note the differences in the projected precipitation changes in the two version of MPI: the HR version shows both further decreases and increases in precipitation in the tropics compared to the LR version, and at high latitudes LR shows much higher changes compared to HR. This shows that even given the same AOD distribution, and similar models, some of the observed changes in the case of SAI may differ depending on the simulated response of the circulation to the same forcing, which in the two versions of MPI could be caused by the different horizontal resolution. In this work we have only analyzed the annual response to precipitation, but there are many regions where changes to the seasonal cycle of precipitation may be even more crucial, such as those that experience a monsoon climate, and whose cycle might be affected by SAI (see for instance Simpson et al. (2019); Visioni et al. (2020b)

for the Indian subcontinent, and Da-Allada et al. (2020) for Western Africa): an in depth analyses of these impacts would also be necessary. Interestingly, unlike for the surface temperatures multi-model standard error (Fig. 6), the one for precipitation is very similar and in some cases higher in G6sulfur than in SSP5-8.5.

This indicates that, while true that reducing surface temperatures would indeed reduce disagreement in future projections between models, that might not hold true for other impacts (of which precipitation might only be an example). For them, due to the influence of changes in surface temperatures, effects driven by CO_2 (both radiative and physiological) and possible changes in dynamical perturbations driven by the aerosols, modeling uncertainties might remain higher either with high CO_2 or with geoengineering. Some of the drivers of uncertainty may be observed by looking at global and land mean precipitation changes in the last 20 years: for the former, the multi-model mean projects an increase of 2.28 ± 0.80 % compared to SSP2-4.5 in the same period, while it projects a decrease of -3.79 ± 0.76 % for G6sulfur (compared to -2.07 ± 0.40 % for G6solar). For the latter, the SSP5-8.5 increase is 1.53 ± 0.73 %, while for G6sulfur the decrease is -3.96 ± 1.50 %, and -2.35 ± 0.79 % (see Fig. S3 for the results of the single models). For both G6sulfur and SSP5-8.5, the spread of the precipitation response over land is much larger compared to G6solar, and depending on the model there are different responses when comparing the global mean versus the land-mean. As this could be due to a variety of factors, future studies should try to understand what is causing these different responses in the various models.
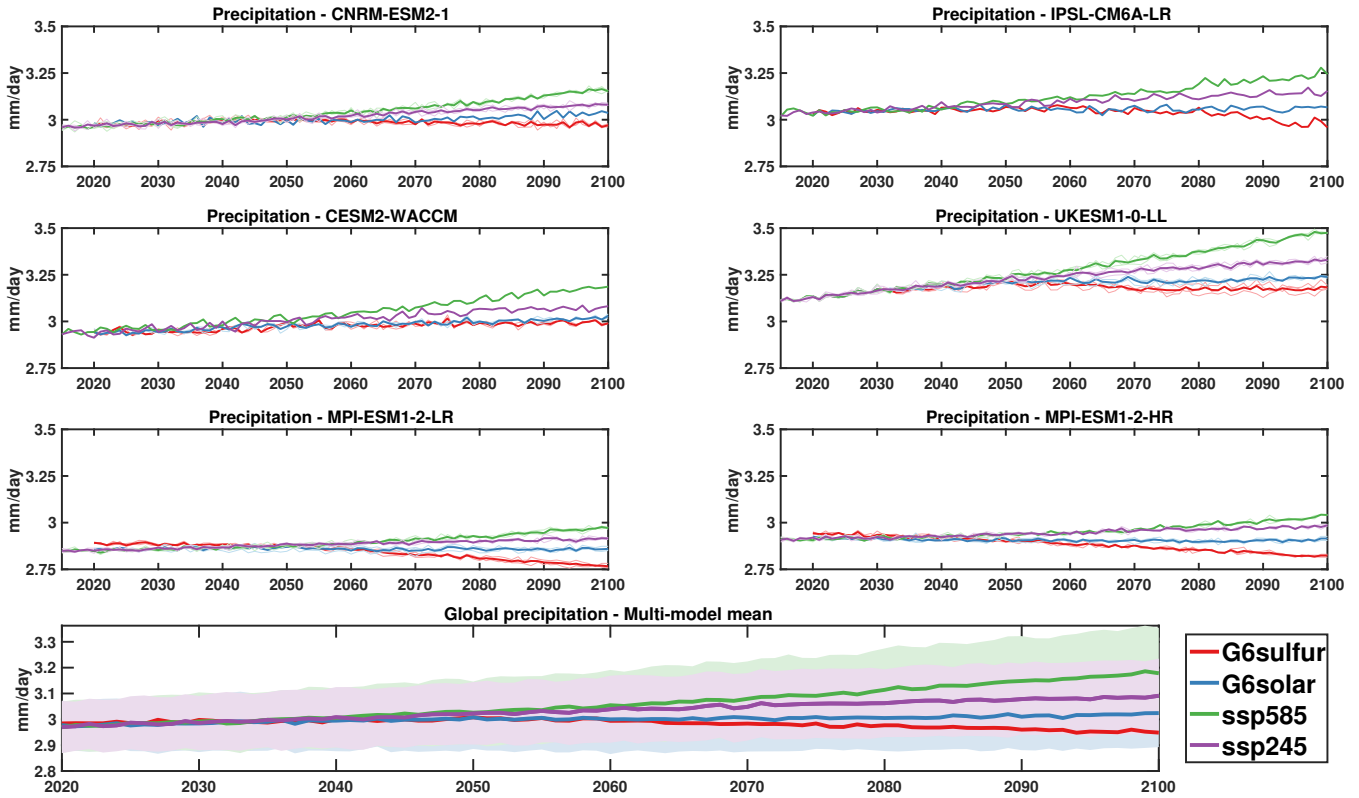
Figure 8. Global mean precipitation (mm/day) for the four experiments for each participating model. The multi-models mean is shown at the bottom, with the shading representing 1σ standard deviation of the mean for each experiment.

Table 1. Summary of model simulations used in this work. The first column has the name of the model used, the DOI for the relative CMIP6 dataset as recommended by CMIP6 (see Stockhause and Lautenschlager (2021)) and the horizontal and vertical resolution, whereas column 2 indicates the main scientific reference where the model version is described. Columns 3 to 6 show the size of the ensemble analyzed in this work: for some models, more ensemble members are available for the SSP experiments, but only those with the same variant as the G6 experiments are used in this work. Finally, the last two columns indicate the source of stratospheric aerosols for G6 and the presence of interactive stratospheric ozone. All models have interactive marine biogeochemistry and are coupled to an interactive land model.

Model name and CMIP6 DOI (resolution[†])	Main scientific reference(s)	SSP2-4.5	SSP5-8.5	G6solar	G6sulfur	Stratospheric aerosols in G6sulfur	Interactive stratospheric ozone
		(number of simulations and variant names)					
CESM2(WACCM) Danabasoglu (2019) h:288×192,v:70	Danabasoglu et al. (2020) Gettelman et al. (2019)	2 r1,r2	2 r1,r2	2 r1,r2	2 r1,r2	From SO_2 injection[‡]	Yes
CNRM-ESM2-1 Seferian (2018) h:256×128,v:40	Séférian et al. (2019)	3 r1,r2,r3	3 r1	1 r1	3 r1,r2,r3	AOD scaled from Tilmes et al. (2015)	Yes Michou et al. (2020)
IPSL-CM6A-LR Boucher et al. (2018) h:144×143,v:79	Boucher et al. (2020) Lurton et al. (2020)	1 r1	1 r1	1 r1	1 r1	From SO_2 injection	No
MPI-ESM1.2-LR Wieners et al. (2019) h:192×96,v:47	Muller et al. (2018)	3 r1,r2,r3	3 r1,r2,r	3 r1,r2,r	3 r1,r2,r3	AOD scaled from Niemeier and Schmidt (2017)	No
MPI-ESM1.2-HR Jungclaus et al. (2019) h:384×192,v:95	Muller et al. (2018)	3 r1,r2,r3	3 r1,r2,r	3 r1,r2,r	3 r1,r2,r	AOD scaled from Niemeier and Schmidt (2017)	No
UKESM1-0-LL Tang et al. (2019) h:192×144,v:85	Sellar et al. (2019)	3 r1,r4,r8	3 r1,r4,r8	3 r1,r4,r8	3 r1,r4,r8	From SO_2 injection	Yes

[†] resolution is described as horizontal (h), lat × lon, and vertical (v). [‡]Injected at the Equator at 25 km in deviation from the protocol described by Kravitz et al. (2015)

Table 2. Summary of results for the simulations in this work for the last two decades of the experiment (2081-2100). When applicable, values are considered as global mean, ensemble mean averages. In the last three columns, the solar reduction needed in the G1 experiment (Kravitz et al. (2020)) to offset the forcing of a $4\times CO_2$ increase, the effective Equilibrium Climate Sensitivity (ECS) from Zelinka et al. (2020) and the Transient Climate Response (TCR) from Meehl et al. (2020) are included for comparison.

Model	ΔT (K) (SSP58.5-SSP24.5)	AOD	Injected SO_2 (Tg-SO_2/yr)	Solar Reduction (G6) (%)	Solar Reduction (G1) (%, Kravitz et al. (2020))	ECS (K) Zelinka et al. (2020)	TCR (K)
CESM2(WACCM)	2.42	0.296	21[†]	2.33	4.91	4.68	2.0
CNRM-ESM2-1	1.90	0.327	N.A.[‡]	1.36	3.72	4.79	1.9
IPSL-CM6A-LR	2.40	0.363	40[†]	1.78	4.10	4.56	2.3
MPI-ESM1.2-LR	1.58	0.235	36[‡]	2.15	4.57	2.98	1.8
MPI-ESM1.2-HR	1.50	0.235	36[‡]	2.15	N.A.	2.98	1.7
UKESM1-0-LL	2.54	0.357	21[†]	2.18	3.80	5.36	2.8
Model average	2.05 ± 0.42 K	0.307 ± 0.061	29 ± 9	1.99 ± 0.36	4.22 ± 1.00	2.1 ± 0.4	

[†] Models using emissions of SO_2. [‡] Models using prescribed AOD.
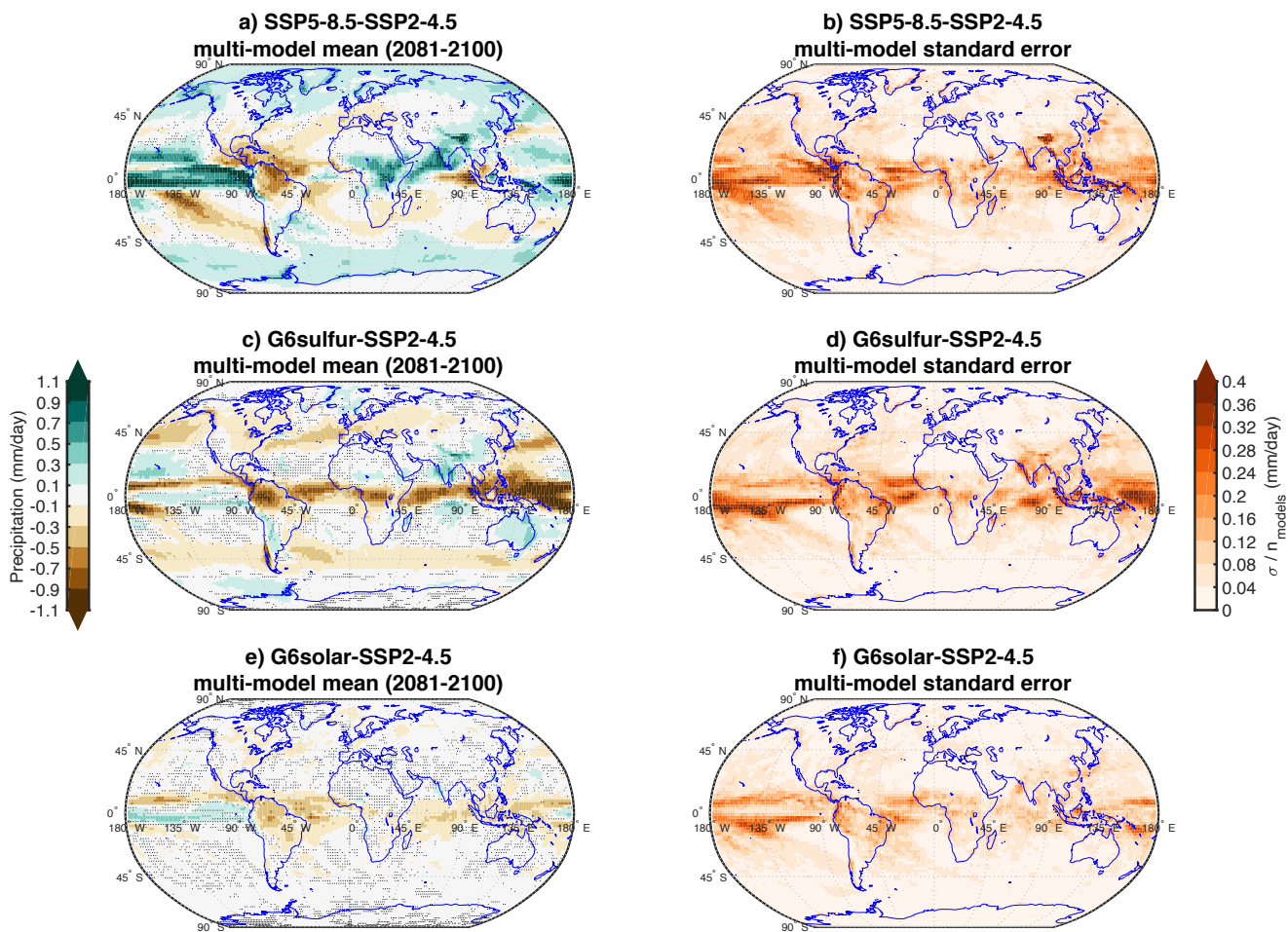
Figure 9. Left column: multi-model averages for precipitation changes averaged over 2081-2100 in different cases (a) SSP5-8.5; c) G6sulfur; e) G6solar) minus the same period for SSP2-4.5. Etched areas (in grey) indicate where less than 66% of models (here, 4 out of 6) agree on the sign of the difference in that grid-point. Right column: Standard error in the multi-model mean for the same reference case on the left. All models results have been re-gridded using a common grid equivalent to that from the model with the lowest horizontal resolution.
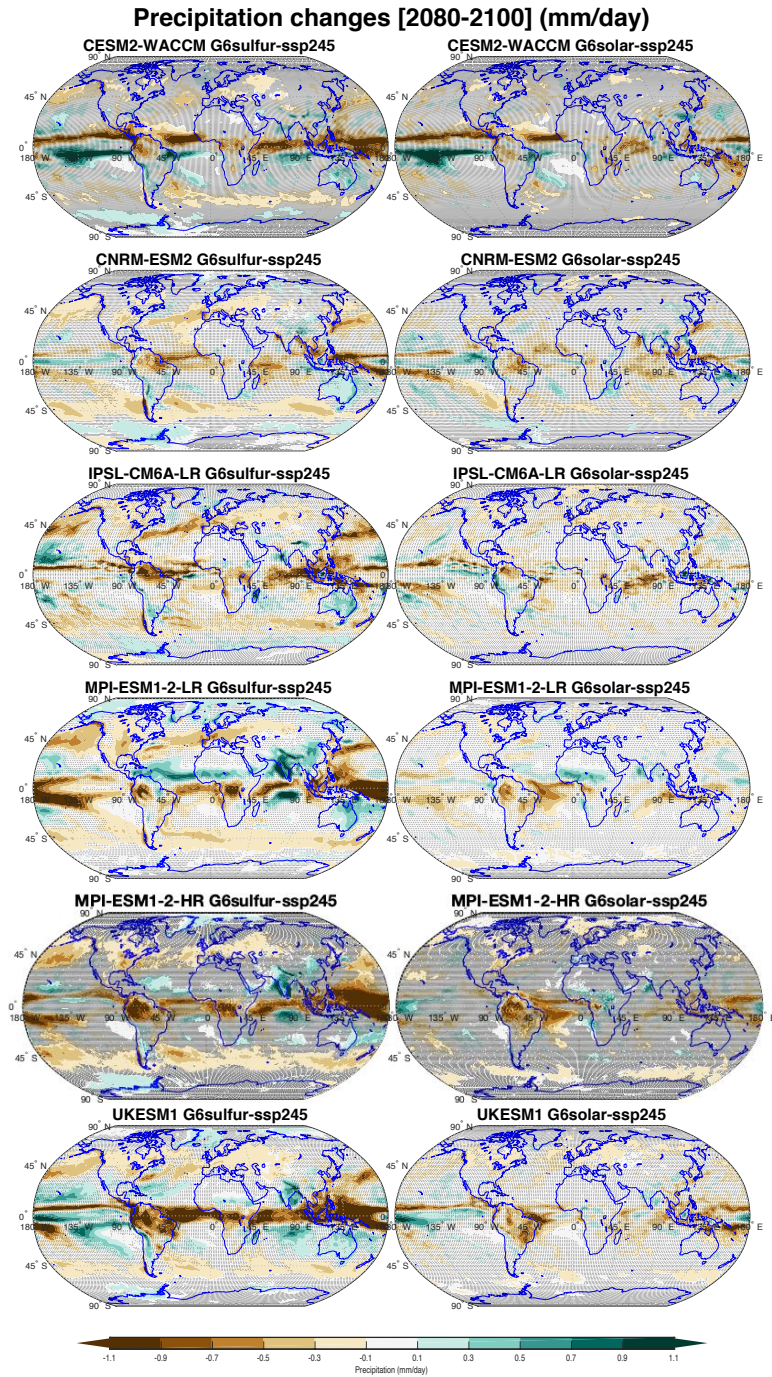
Figure 10. Precipitation changes (mm/day) in the period 2081-2100 in G6sulfur compared to the same period for SSP2-4.5 in G6sulfur (left panels) simulations and G6solar simulations (right panels) for all participating models. Shaded areas indicate where the difference is not statistically significant, evaluated using a double-sided t-test with p<0.05, considering all 20 years as independent samples.
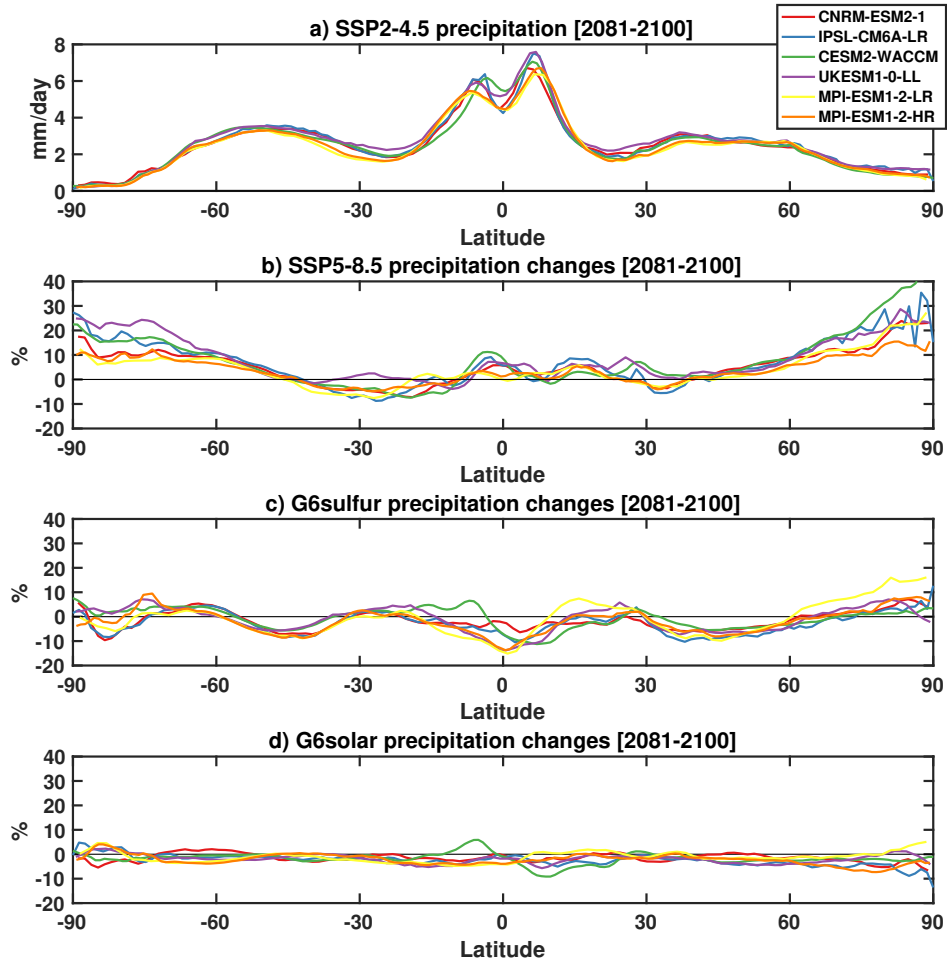
Figure 11. a) Zonal mean precipitation (mm/day) in the period 2081-2100 in SSP2-4.5. b) Precipitation changes (%) compared to SSP2-4.5 in the same period for SSP5-8.5. c-d) as in b), but for G6sulfur and G6solar respectively.

4 Conclusions

We have shown in this work some preliminary results from the G6sulfur and G6solar modeling experiments, proposed in Kravitz et al. (2015) for the Geoengineering Model Intercomparison Project, part of the Climate Model Intercomparison Project Phase 6. These two new experiments aim to reduce global temperatures in the 21st century from those simulated under a high-tier emissions scenario (SSP5-8.5) to those simulated under a medium-tier emissions scenario (SSP2-4.5), either by simulating the artificial injection of stratospheric aerosol precursors in the stratosphere, or by reducing the solar constant in the models. In terms of surface climate response, some broad features are shared by all models, such as a reduction in global mean precipitation compared to both SSP scenarios, and a residual warming in the northern high latitudes (Henry and Merlis (2020)), particularly present in G6sulfur (Simpson et al. (2019); Banerjee et al. (2020)). Other locations show more disagreements between models in terms of the surface temperature response. Since there is a larger uniformity in the response between G6solar simulations, where the solar dimming is applied in the same latitudinally-uniform way in all models, this suggests that part of the surface response uncertainty in G6sulfur is driven by differences in the latitudinal distribution of the aerosols and not to a different response of the surface climate to the same radiative forcing.

The comparison of the two experiments may help in various ways: when comparing the single-model response to the two different forcings, it helps highlight some of the physical differences between the two interventions (as in Visioni et al. (2021)), produced by the the stratospheric aerosols physical and chemical effects. Analysing the inter-model spread also highlights the degree to which uncertainty in surface climate response to stratospheric aerosols is driven by uncertainties in the stratospheric processes, versus uncertainties in how the climate response to a specified forcing such as reduced insolation, and may point to a path to successfully identify and, eventually, reduce some of them. We have shown that large inter-model variability remains in the distribution of the aerosol after injections of SO_2 in the tropical stratosphere, as well as in the temperature response of the stratosphere. As we discussed in Section 3.2, the resulting latitudinal distribution of the aerosols given similar injection locations can be due to multiple factors; for instance, the stratospheric dynamics differences regulating the large-scale transport of the aerosols, and the microphysical differences regulating the oxidation of SO_2 and the subsequent growth of the aerosols. The interaction between the stratospheric aerosols and the rest of the system further complicates the identification of a single mechanism by which to aerosol distributions might differ: there may be uncertainties related to the simulated radiative interaction (for instance, the rate of absorption of IR radiation by the aerosols) and stratospheric chemistry (i.e., changes in ozone chemistry, which in turns affect local radiative transfer) that may produce different localized heating of air and thus affect differently both the surface climate and stratospheric dynamics (which, in turn, may affect the aerosol distribution, Niemeier and Schmidt (2017); Kleinschmitt et al. (2018)). All these uncertainties in stratospheric dynamics (summarized in Fig.12) can thus indirectly affect surface climate in simulations of geoengineering with stratospheric aerosols, by means of a different reflection of sunlight depending on the resulting distribution of the aerosols. This type of uncertainty is thus separated from those directly connected to a stratospheric influence on various aspects of the surface climate: local surface temperatures (Jiang et al. (2019)),

precipitation (Simpson et al. (2019)) or cloud cover changes (Visioni et al. (2018a)).

430

Simulations such as those we analyzed here can give useful information on the current range of uncertainty over many projected impacts of geoengineering. In particular, the successful coupling of the new Earth System Models used in CMIP6 with land, ocean and cryosphere components can help with the exploration of various impacts, for instance on ecosystems (Zarnetske et al. (2021)) or ice sheets melting (Fettweis et al. (2020)), which are crucial to properly inform policymakers and interested parties, and the inter-model spread can help in communicating the uncertainties tied to those projections. As we outlined above, however, these simulations may not be as useful in helping reduce most of these uncertainties: it is therefore important not to rely only on these simulations going forward, but to devise new experiments that might improve the accuracy with which we model the relevant interactions in the atmosphere. To do so, there may be multiple venues: one way could be using different physical-based approaches to modeling that don't involve 3D climate modeling and that might shed light on the single processes (i.e. for instance Dai et al. (2018); Lutsko et al. (2020); Seeley et al. (2021), or plume modeling), lab experiments trying to replicate the conditions of the stratosphere (Dai et al. (2020)). Another way could be using global climate models but trying to constrain some of the various processes in order to reduce uncertainty: this could be done, for instance, by prescribing the same stratospheric aerosol distribution in different models (as suggested in Tilmes et al. (2015)) and as some models do in this work, or modifying some parameters in the model simulation while keeping everything else fixed to constrain a source of uncertainty (as proposed for volcanic eruption by Timmreck et al. (2018) in the Pinatubo Emulation in Multiple models (PoEMs) experiment), or by continuing to simulate a constant solar dimming in place of the more complex aerosols (see for instance Irvine et al. (2019)) to understand portions of the global surface response. All of these methods combined (and more), may be able to increase our confidence when projecting the impacts of sulfate geoengineering as a short-term addition to mitigation (but not as its replacement, MacMartin et al. (2018); de Coninck et al. (2018)) in order to limit the harmful impacts of climate change.

When considering the possible impacts of SAI using GeoMIP simulations, it should also be considered that the injection strategy simulated in the G6 experiments is only one of the possible ways in which SAI could be deployed, and for various reasons, it may not even be the most ideal. Kravitz et al. (2019) showed that a strategy that makes use of different locations of injection outside the equator (MacMartin et al. (2017)) in order to manage not just global mean temperatures, but also inter-hemispheric and equator-to-pole temperature gradients, would further reduce harmful impacts by better restoring sea-ice and maintain the ITCZ location. Further, injecting all days of the year might also not be the most ideal choice (Visioni et al. (2019)), and some of the resulting climatic effects might depend on the seasonal distribution of the aerosol cloud (Visioni et al. (2020b)). So, while the coordinated experiment described in this work might be good as a starting point, it should not be considered as the only way in which SAI might be deployed. This is also valid in terms of the underlying emission scenario used, as a future where emissions continue unabated (as SSP5-8.5, the scenario used for the G6 experiments, is) is absolutely not the ideal one in which an eventual SAI deployment should be imagined, even if it might mitigate the short-term effects of the GHG-induced warming. A scenario where emissions are cut, but not fast enough, and global temperature thresholds set by

Main physical sources of uncertainties for Sulfate Geoengineering
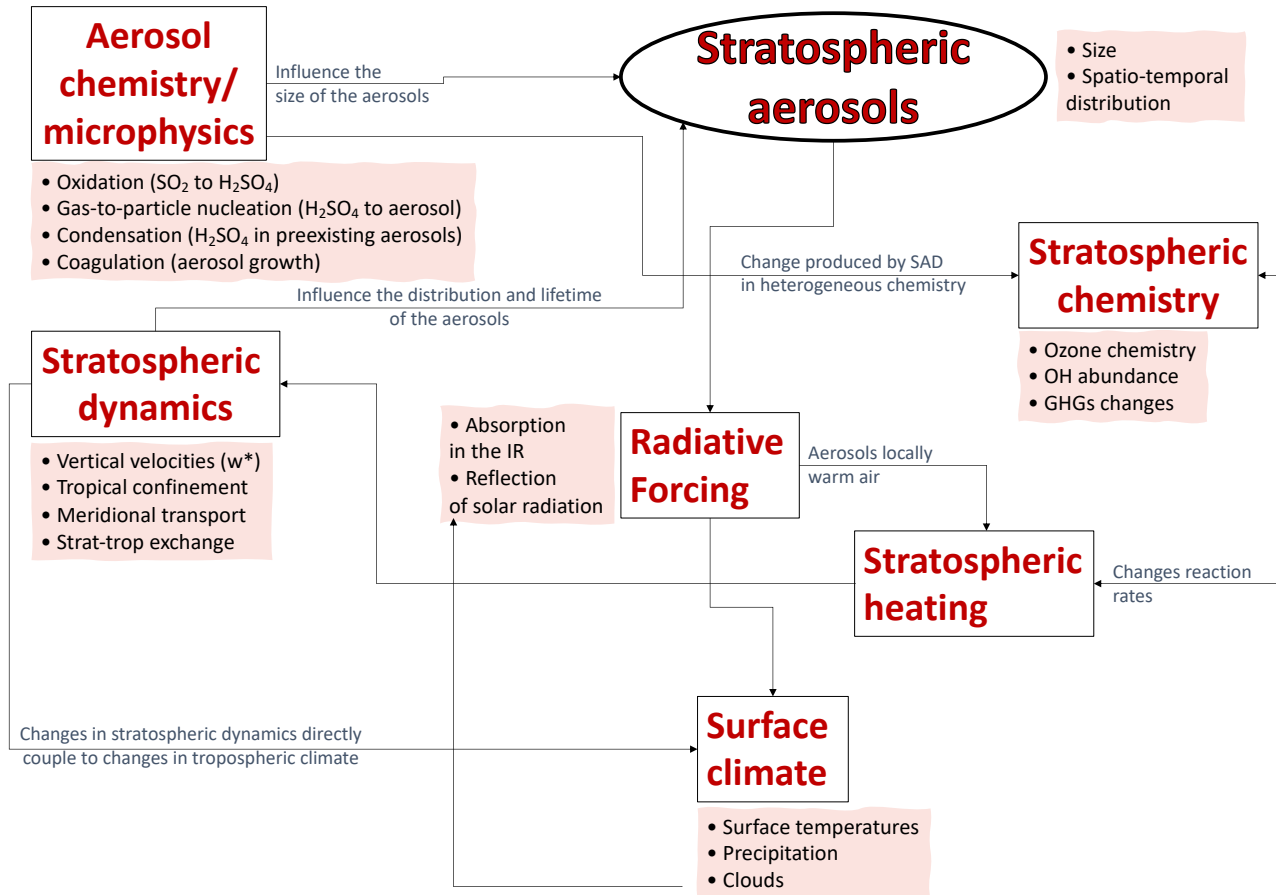
Figure 12. Scheme exemplifying the sources of uncertainties in modeling stratospheric aerosols in the context of sulfate geoengineering. Components of the Earth System (and more more particularly, of the atmosphere; i.e., Stratospheric dynamics) are in boxes: for each of them, the main processes that would affect (and be affected by) the injection of SO_2 in the stratosphere are listed (red shading), and interactions between components are represented by arrows, with an explanation in grey. "Stratospheric aerosols" and "Stratospheric heating" are in circles to distinguish them from underlying system components, as they can be considered a single component that is affected and affects multiple things in turn.

international agreements may be temporarily exceeded could be one where a limited deployment of SAI might be considered
465   as a short-term mitigation strategy, with more limited consequences on the environment (Tilmes et al. (2020)).

Code and data availability. All data used in this work is available from the Earth System Grid (https://esgf-node.llnl.gov/search/cmip6/)

Author contributions. DV performed the analyses and wrote the manuscript. DGM and BK helped with analyses and advised DV through-
out the writing process. OB, AJ, LT, MM, MJM, PN, UN, RS and ST performed the simulations and offered valuable comments on the
manuscript.

470   *Competing interests.* The authors declare no competing interests.

Acknowledgements. Support for DGM was provided by the National Science Foundation through agreement CBET-1818759. Support for
DV was provided by the Atkinson Center for a Sustainable Future at Cornell University. Support for BK was provided in part by the National
Sciences Foundation through agreement CBET-1931641, the Indiana University Environmental Resilience Institute, and the Prepared for En-
vironmental Change Grand Challenge initiative. The Pacific Northwest National Laboratory is operated for the U.S. Department of Energy
475   by Battelle Memorial Institute under contract DE-AC05-76RL01830. This work benefited from the French state aid managed by the ANR
under the "Investissements d'avenir" programme with the reference ANR-11-IDEX-0004-17-EURE-0006. AJ was supported by the Met
Office Hadley Centre Climate Programme funded by the UK Government Department for Business, Energy and Industrial Strategy (BEIS)
and the UK Government Department for Environment, Food and Rural Affairs (Defra). UN has been supported by the Deutsche Forschungs-
gemeinschaft Research Unit VollImpact (FOR2820). MM,PN, OB and RS acknowledge support from the European Union's Horizon 2020
480   research and innovation programme under grant agreement No 820829 (CONSTRAIN) and thank the support of the team in charge of the
CNRM-CM climate model. MPI-ESM were performed on the computer of Deutsches Klima Rechenzentrum (DKRZ). The CESM project
is supported primarily by the National Science Foundation. The IPSL-CM6 experiments were performed using the HPC resources of TGCC
under the allocations 2019-A0060107732 and 2020-A0080107732 (project gencmip6) provided by GENCI (Grand Equipement National de
Calcul Intensif). Supercomputing time for CNRM-ESM-2 was provided by the Meteo-France/DSI supercomputing center.

References

Aquila, V., Garfinkel, C., Newman, P., Oman, L., and Waugh, D.: Modifications of the quasi-biennial oscillation by a geoengineering perturbation of the stratospheric aerosol layer, Geophysical Research Letters, 41, 1738–1744, 2014.

Arora, V. K., Katavouta, A., Williams, R. G., Jones, C. D., Brovkin, V., Friedlingstein, P., Schwinger, J., Bopp, L., Boucher, O., Cadule, P., Chamberlain, M. A., Christian, J. R., Delire, C., Fisher, R. A., Hajima, T., Ilyina, T., Joetzjer, E., Kawamiya, M., Koven, C. D., Krasting, J. P., Law, R. M., Lawrence, D. M., Lenton, A., Lindsay, K., Pongratz, J., Raddatz, T., Séférian, R., Tachiiri, K., Tjiputra, J. F., Wiltshire, A., Wu, T., and Ziehn, T.: Carbon–concentration and carbon–climate feedbacks in CMIP6 models and their comparison to CMIP5 models, Biogeosciences, 17, 4173–4222, 2020.

Aswathy, V. N., Boucher, O., Quaas, M., Niemeier, U., Muri, H., Mulmenstadt, J., and Quaas, J.: Climate extremes in multi-model simulations of stratospheric aerosol and marine cloud brightening climate engineering, Atmospheric Chemistry and Physics, 15, 9593–9610, https://doi.org/10.5194/acp-15-9593-2015, https://acp.copernicus.org/articles/15/9593/2015/, 2015.

Ban-Weiss, G. A. and Caldeira, K.: Geoengineering as an optimization problem, Environmental Research Letters, 5, https://doi.org/10.1088/1748-9326/5/3/034009, 2010.

Banerjee, A., Butler, A. H., Polvani, L. M., Robock, A., Simpson, I. R., and Sun, L.: Robust winter warming over Eurasia under stratospheric sulfate geoengineering – the role of stratospheric dynamics, Atmospheric Chemistry and Physics Discussions, 2020, 1–20, https://doi.org/10.5194/acp-2020-965, https://acp.copernicus.org/preprints/acp-2020-965/, 2020.

Boucher, O., Kleinschmitt, C., and Myhre, G.: Quasi-Additivity of the Radiative Effects of Marine Cloud Brightening and Stratospheric Sulfate Aerosol Injection, Geophysical Research Letters, 44, 11,158–11,165, https://doi.org/https://doi.org/10.1002/2017GL074647, https://agupubs.onlinelibrary.wiley.com/doi/abs/10.1002/2017GL074647, 2017.

Boucher, O., Denvil, S., Levavasseur, G., Cozic, A., Caubel, A., Foujols, M.-A., Meurdesoif, Y., Cadule, P., Devilliers, M., Ghattas, J., Lebas, N., Lurton, T., Mellul, L., Musat, I., Mignot, J., and Cheruy, F.: IPSL IPSL-CM6A-LR model output prepared for CMIP6 CMIP historical, https://doi.org/10.22033/ESGF/CMIP6.5195, https://doi.org/10.22033/ESGF/CMIP6.5195, 2018.

Boucher, O., Servonnat, J., Albright, A. L., Aumont, O., Balkanski, Y., Bastrikov, V., Bekki, S., Bonnet, R., Bony, S., Bopp, L., Braconnot, P., Brockmann, P., Cadule, P., Caubel, A., Cheruy, F., Codron, F., Cozic, A., Cugnet, D., D'Andrea, F., Davini, P., de Lavergne, C., Denvil, S., Deshayes, J., Devilliers, M., Ducharne, A., Dufresne, J.-L., Dupont, E., Éthé, C., Fairhead, L., Falletti, L., Flavoni, S., Foujols, M.-A., Gardoll, S., Gastineau, G., Ghattas, J., Grandpeix, J.-Y., Guenet, B., Guez, Lionel, E., Guilyardi, E., Guimberteau, M., Hauglustaine, D., Hourdin, F., Idelkadi, A., Joussaume, S., Kageyama, M., Khodri, M., Krinner, G., Lebas, N., Levavasseur, G., Lévy, C., Li, L., Lott, F., Lurton, T., Luyssaert, S., Madec, G., Madeleine, J.-B., Maignan, F., Marchand, M., Marti, O., Mellul, L., Meurdesoif, Y., Mignot, J., Musat, I., Ottlé, C., Peylin, P., Planton, Y., Polcher, J., Rio, C., Rochetin, N., Rousset, C., Sepulchre, P., Sima, A., Swingedouw, D., Thiéblemont, R., Traore, A. K., Vancoppenolle, M., Vial, J., Vialard, J., Viovy, N., and Vuichard, N.: Presentation and Evaluation of the IPSL-CM6A-LR Climate Model, Journal of Advances in Modeling Earth Systems, 12, e2019MS002 010, https://doi.org/10.1029/2019MS002010, https://agupubs.onlinelibrary.wiley.com/doi/abs/10.1029/2019MS002010, e2019MS002010 10.1029/2019MS002010, 2020.

Budyko, M. I.: The Climate of the Future, American Geophysical Union, https://doi.org/10.1002/9781118665251.ch7, http://dx.doi.org/10.1002/9781118665251.ch7, 1978.

Canty, T., Mascioli, N. R., Smarte, M. D., and Salawitch, R. J.: An empirical model of global climate – Part 1: A critical evaluation of volcanic cooling, Atmospheric Chemistry and Physics, 13, 3997–4031, 2013.

Cheng, W., MacMartin, D. G., Dagon, K., Kravitz, B., Tilmes, S., Richter, J. H., Mills, M. J., and Simpson, I. R.: Soil Moisture and Other Hydrological Changes in a Stratospheric Aerosol Geoengineering Large Ensemble, Journal of Geophysical Research: Atmospheres, 124, 12 773–12 793, https://doi.org/10.1029/2018JD030237, https://agupubs.onlinelibrary.wiley.com/doi/abs/10.1029/2018JD030237, 2019.

525 Clyne, M., Lamarque, J.-F., Mills, M. J., Khodri, M., Ball, W., Bekki, S., Dhomse, S. S., Lebas, N., Mann, G., Marshall, L., Niemeier, U., Poulain, V., Robock, A., Rozanov, E., Schmidt, A., Stenke, A., Sukhodolov, T., Timmreck, C., Toohey, M., Tummon, F., Zanchettin, D., Zhu, Y., and Toon, O. B.: Model physics and chemistry causing intermodel disagreement within the VolMIP-Tambora Interactive Stratospheric Aerosol ensemble, Atmospheric Chemistry and Physics Discussions, 2020, 1–43, https://doi.org/10.5194/acp-2020-883, https://acp.copernicus.org/preprints/acp-2020-883/, 2020.

Crutzen, P. J.: Albedo Enhancement by Stratospheric Sulfur Injections: A Contribution to Resolve a Policy Dilemma?, Climatic Change, 77,
530 211–220, https://doi.org/10.1007/s10584-006-9101-y, http://dx.doi.org/10.1007/s10584-006-9101-y, 2006.

Da-Allada, C. Y., Baloïtcha, E., Alamou, E. A., Awo, F. M., Bonou, F., Pomalegni, Y., Biao, E. I., Obada, E., Zandagba, J. E., Tilmes, S., and Irvine, P. J.: Changes in West African Summer Monsoon Precipitation Under Stratospheric Aerosol Geoengineering, Earth's Future, 8, e2020EF001 595, https://doi.org/https://doi.org/10.1029/2020EF001595, https://agupubs.onlinelibrary.wiley.com/doi/abs/10.1029/2020EF001595, e2020EF001595 2020EF001595, 2020.

535 Dai, Z., Weisenstein, D. K., and Keith, D. W.: Tailoring Meridional and Seasonal Radiative Forcing by Sulfate Aerosol Solar Geoengineering, Geophysical Research Letters, 45, 1030–1039, https://doi.org/10.1002/2017GL076472, 2018.

Dai, Z., Weisenstein, D. K., Keutsch, F. N., and Keith, D. W.: Experimental reaction rates constrain estimates of ozone response to calcium carbonate geoengineering, Communications Earth & Environment, 1, 63, 2020.

Danabasoglu, G.: NCAR CESM2-WACCM model output prepared for CMIP6 CMIP, https://doi.org/10.22033/ESGF/CMIP6.10024, https:
540 //doi.org/10.22033/ESGF/CMIP6.10024, 2019.

Danabasoglu, G., Lamarque, J.-F., Bacmeister, J., Bailey, D. A., DuVivier, A. K., Edwards, J., Emmons, L. K., Fasullo, J., Garcia, R., Gettelman, A., Hannay, C., Holland, M. M., Large, W. G., Lauritzen, P. H., Lawrence, D. M., Lenaerts, J. T. M., Lindsay, K., Lipscomb, W. H., Mills, M. J., Neale, R., Oleson, K. W., Otto-Bliesner, B., Phillips, A. S., Sacks, W., Tilmes, S., van Kampenhout, L., Vertenstein, M., Bertini, A., Dennis, J., Deser, C., Fischer, C., Fox-Kemper, B., Kay, J. E., Kinnison, D., Kushner, P. J., Larson, V. E., Long, M. C.,
545 Mickelson, S., Moore, J. K., Nienhouse, E., Polvani, L., Rasch, P. J., and Strand, W. G.: The Community Earth System Model Version 2 (CESM2), Journal of Advances in Modeling Earth Systems, 12, e2019MS001 916, https://doi.org/10.1029/2019MS001916, https://agupubs.onlinelibrary.wiley.com/doi/abs/10.1029/2019MS001916, e2019MS001916 2019MS001916, 2020.

de Coninck, H., Revi, A., Babiker, M., Bertoldi, P., Buckeridge, M., Cartwright, A., Dong, W., Ford, J., Fuss, S., Hourcade, J.-C., Ley, D., Mechler, R., Newman, P., Revokatova, A., Schultz, S., Steg, L., and Sugiyama, T.: Chapter 4: Strengthening and Implementing the Global
550 Response, in: Global warming of 1.5°C. An IPCC Special Report on the impacts of global warming of 1.5°C above pre-industrial levels and related global greenhouse gas emission pathways, in the context of strengthening the global response to the threat of climate change, sustainable development, and efforts to eradicate poverty, edited by IPCC, IPCC, https://www.ipcc.ch/sr15/chapter/chapter-4/, 2018.

Dhomse, S. S., Mann, G. W., Antuña Marrero, J. C., Shallcross, S. E., Chipperfield, M. P., Carslaw, K. S., Marshall, L., Abraham, N. L., and Johnson, C. E.: Evaluating the simulated radiative forcings, aerosol properties, and stratospheric warmings from the 1963
555 Mt Agung, 1982 El Chichón, and 1991 Mt Pinatubo volcanic aerosol clouds, Atmospheric Chemistry and Physics, 20, 13 627–13 654, https://doi.org/10.5194/acp-20-13627-2020, https://acp.copernicus.org/articles/20/13627/2020/, 2020.

Duan, L., Cao, L., Bala, G., and Caldeira, K.: Climate Response to Pulse Versus Sustained Stratospheric Aerosol Forcing, Geophysical Research Letters, 46, 8976–8984, https://doi.org/https://doi.org/10.1029/2019GL083701, https://agupubs.onlinelibrary.wiley.com/doi/abs/10.1029/2019GL083701, 2019.

560 Fasullo, J. T., Simpson, I. R., Kravitz, B., Tilmes, S., Richter, J. H., MacMartin, D. G., and Mills, M. J.: Persistent polar ocean warming in a strategically geoengineered climate, Nature Geoscience, 11, 910–914, https://doi.org/10.1038/s41561-018-0249-7, http://dx.doi.org/10.1038/s41561-018-0249-7, 2018.

Fettweis, X., Hofer, S., Seferian, R., Amory, C., Delhasse, A., Doutreloup, S., Kittel, C., Lang, C., Van Bever, J., Veillon, F., and Irvine, P.: Brief Communication: "Reduction of the future Greenland ice sheet surface melt with the help of solar geoengineering", The Cryosphere

565 Discussions, 2020, 1–10, https://doi.org/10.5194/tc-2020-347, https://tc.copernicus.org/preprints/tc-2020-347/, 2020.

Franke, H., Niemeier, U., and Visioni, D.: Differences in the QBO response to stratospheric aerosol modification depending on injection strategy and species, Atmospheric Chemistry and Physics Discussions, 2020, 1–29, https://doi.org/10.5194/acp-2020-1104, https://acp.copernicus.org/preprints/acp-2020-1104/, 2020.

Gettelman, A., Hannay, C., Bacmeister, J. T., Neale, R. B., Pendergrass, A. G., Danabasoglu, G., Lamarque, J.-F., Fasullo, J. T., Bailey,

570 D. A., Lawrence, D. M., and Mills, M. J.: High Climate Sensitivity in the Community Earth System Model Version 2 (CESM2), Geophysical Research Letters, 46, 8329–8337, https://doi.org/10.1029/2019GL083978, https://agupubs.onlinelibrary.wiley.com/doi/abs/10.1029/2019GL083978, 2019.

Glienke, S., Irvine, P. J., and Lawrence, M. G.: The impact of geoengineering on vegetation in experiment G1 of the GeoMIP, Journal of Geophysical Research: Atmospheres, 120, 10,196–10,213, https://doi.org/10.1002/2015JD024202, https://agupubs.onlinelibrary.wiley.

575 com/doi/abs/10.1002/2015JD024202, 2015.

Govindasamy, B., Caldeira, K., and Duffy, P.: Geoengineering Earth's radiation balance to mitigate climate change from a quadrupling of CO2, Global and Planetary Change, 37, 157 – 168, https://doi.org/https://doi.org/10.1016/S0921-8181(02)00195-9, http://www.sciencedirect.com/science/article/pii/S0921818102001959, evaluation, Intercomparison and Application of Global Climate Models, 2003.

Hansen, J., Sato, M., Ruedy, R., Nazarenko, L., Lacis, A., Schmidt, G. A., Russell, G., Aleinov, I., Bauer, M., Bauer, S., Bell, N., Cairns, B.,

580 Canuto, V., Chandler, M., Cheng, Y., Del Genio, A., Faluvegi, G., Fleming, E., Friend, A., Hall, T., Jackman, C., Kelley, M., Kiang, N., Koch, D., Lean, J., Lerner, J., Lo, K., Menon, S., Miller, R., Minnis, P., Novakov, T., Oinas, V., Perlwitz, J., Perlwitz, J., Rind, D., Romanou, A., Shindell, D., Stone, P., Sun, S., Tausnev, N., Thresher, D., Wielicki, B., Wong, T., Yao, M., and Zhang, S.: Efficacy of climate forcings, Journal of Geophysical Research: Atmospheres, 110, https://doi.org/10.1029/2005JD005776, https://agupubs.onlinelibrary.wiley.com/doi/abs/10.1029/2005JD005776, 2005.

585 Henry, M. and Merlis, T. M.: Forcing Dependence of Atmospheric Lapse Rate Changes Dominates Residual Polar Warming in Solar Radiation Management Climate Scenarios, Geophysical Research Letters, 47, e2020GL087 929, https://doi.org/10.1029/2020GL087929, https://agupubs.onlinelibrary.wiley.com/doi/abs/10.1029/2020GL087929, e2020GL087929 10.1029/2020GL087929, 2020.

Irvine, P., Emanuel, K., He, J., Horowitz, L. W., Vecchi, G., and Keith, D.: Halving warming with idealized solar geoengineering moderates key climate hazards, Nature Climate Change, 9, 295–299, https://doi.org/10.1038/s41558-019-0398-8, http://dx.doi.org/10.1038/

590 s41558-019-0398-8, 2019.

Irvine, P. J. and Keith, D. W.: Halving warming with stratospheric aerosol geoengineering moderates policy-relevant climate hazards, Environmental Research Letters, 15, 044 011, https://doi.org/10.1088/1748-9326/ab76de, 2020.

Ji, D., Fang, S., Curry, C. L., Kashimura, H., Watanabe, S., Cole, J. N. S., Lenton, A., Muri, H., Kravitz, B., and Moore, J. C.: Extreme temperature and precipitation response to solar dimming and stratospheric aerosol geoengineering, Atmospheric Chemistry and Physics, 18, 10 133–10 156, https://doi.org/10.5194/acp-18-10133-2018, https://www.atmos-chem-phys.net/18/10133/2018/, 2018.

Jiang, J., Cao, L., MacMartin, D. G., Simpson, I. R., Kravitz, B., Cheng, W., Visioni, D., Tilmes, S., Richter, J. H., and Mills, M. J.: Stratospheric Sulfate Aerosol Geoengineering Could Alter the High-Latitude Seasonal Cycle, Geophysical Research Letters, 46, 14 153–14 163, https://doi.org/10.1029/2019GL085758, 2019.

Jones, A., Haywood, J. M., Jones, A. C., Tilmes, S., Kravitz, B., and Robock, A.: North Atlantic Oscillation response in GeoMIP experiments G6solar and G6sulfur: why detailed modelling is needed for understanding regional implications of solar radiation management, Atmospheric Chemistry and Physics, 21, 1287–1304, https://doi.org/10.5194/acp-21-1287-2021, https://acp.copernicus.org/articles/21/1287/2021/, 2021.

Jones, A. C., Hawcroft, M. K., Haywood, J. M., Jones, A., Guo, X., and Moore, J. C.: Regional Climate Impacts of Stabilizing Global Warming at 1.5 K Using Solar Geoengineering, Earth's Future, 6, 230–251, https://doi.org/10.1002/2017EF000720, 2018.

Jungclaus, J., Bittner, M., Wieners, K.-H., Wachsmann, F., Schupfner, M., Legutke, S., Giorgetta, M., Reick, C., Gayler, V., Haak, H., de Vrese, P., Raddatz, T., Esch, M., Mauritsen, T., von Storch, J.-S., Behrens, J., Brovkin, V., Claussen, M., Crueger, T., Fast, I., Fiedler, S., Hagemann, S., Hohenegger, C., Jahns, T., Kloster, S., Kinne, S., Lasslop, G., Kornblueh, L., Marotzke, J., Matei, D., Meraner, K., Mikolajewicz, U., Modali, K., Müller, W., Nabel, J., Notz, D., Peters, K., Pincus, R., Pohlmann, H., Pongratz, J., Rast, S., Schmidt, H., Schnur, R., Schulzweida, U., Six, K., Stevens, B., Voigt, A., and Roeckner, E.: MPI-M MPI-ESM1.2-HR model output prepared for CMIP6 CMIP historical, https://doi.org/10.22033/ESGF/CMIP6.6594, https://doi.org/10.22033/ESGF/CMIP6.6594, 2019.

Kashimura, H., Abe, M., Watanabe, S., Sekiya, T., Ji, D., Moore, J. C., Cole, J. N. S., and Kravitz, B.: Shortwave radiative forcing, rapid adjustment, and feedback to the surface by sulfate geoengineering: analysis of the Geoengineering Model Intercomparison Project G4 scenario, Atmospheric Chemistry and Physics, 17, 3339–3356, https://doi.org/10.5194/acp-17-3339-2017, https://acp.copernicus.org/articles/17/3339/2017/, 2017.

Kleinschmitt, C., Boucher, O., and Platt, U.: Sensitivity of the radiative forcing by stratospheric sulfur geoengineering to the amount and strategy of the SO2 injection studied with the LMDZ-S3A model, Atmospheric Chemistry and Physics, 18, 2769–2786, https://doi.org/10.5194/acp-18-2769-2018, https://www.atmos-chem-phys.net/18/2769/2018/, 2018.

Kravitz, B. and MacMartin, D. G.: Uncertainty and the basis for confidence in solar geoengineering research, Nature Reviews Earth & Environment, 1, 64–75, https://doi.org/10.1038/s43017-019-0004-7, http://dx.doi.org/10.1038/s43017-019-0004-7{%}0Ahttp://www.nature.com/articles/s43017-019-0004-7, 2020.

Kravitz, B., Robock, A., Boucher, O., Schmidt, H., Taylor, K. E., Stenchikov, G., and Schulz, M.: The Geoengineering Model Intercomparison Project (GeoMIP), Atmospheric Science Letters, 12, 162–167, https://doi.org/10.1002/asl.316, https://rmets.onlinelibrary.wiley.com/doi/abs/10.1002/asl.316, 2011.

Kravitz, B., Caldeira, K., Boucher, O., Robock, A., Rasch, P. J., Alterskjær, K., Karam, D. B., Cole, J. N. S., Curry, C. L., Haywood, J. M., Irvine, P. J., Ji, D., Jones, A., Kristjánsson, J. E., Lunt, D. J., Moore, J. C., Niemeier, U., Schmidt, H., Schulz, M., Singh, B., Tilmes, S., Watanabe, S., Yang, S., and Yoon, J.-H.: Climate model response from the Geoengineering Model Intercomparison Project (GeoMIP), Journal of Geophysical Research: Atmospheres, 118, 8320–8332, https://doi.org/10.1002/jgrd.50646, https://agupubs.onlinelibrary.wiley.com/doi/abs/10.1002/jgrd.50646, 2013a.

Kravitz, B., Rasch, P. J., Forster, P. M., Andrews, T., Cole, J. N., Irvine, P. J., Ji, D., Kristjánsson, J. E., Moore, J. C., Muri, H., Niemeier, U., Robock, A., Singh, B., Tilmes, S., Watanabe, S., and Yoon, J. H.: An energetic perspective on hydrological cycle

changes in the Geoengineering Model Intercomparison Project, Journal of Geophysical Research Atmospheres, 118, 13,087–13,102, https://doi.org/10.1002/2013JD020502, 2013b.

Kravitz, B., Robock, A., Tilmes, S., Boucher, O., English, J. M., Irvine, P. J., Jones, A., Lawrence, M. G., MacCracken, M., Muri, H., Moore, J. C., Niemeier, U., Phipps, S. J., Sillmann, J., Storelvmo, T., Wang, H., and Watanabe, S.: The Geoengineering Model Inter-
comparison Project Phase 6 (GeoMIP6): simulation design and preliminary results, Geoscientific Model Development, 8, 3379–3392, https://doi.org/10.5194/gmd-8-3379-2015, https://gmd.copernicus.org/articles/8/3379/2015/, 2015.

Kravitz, B., MacMartin, D. G., Wang, H., and Rasch, P. J.: Geoengineering as a design problem, Earth System Dynamics, 7, 469–497, https://doi.org/10.5194/esd-7-469-2016, 2016.

Kravitz, B., Lamarque, J.-F., Tribbia, J. J., Tilmes, S., Vitt, F., Richter, J. H., MacMartin, D. G., and Mills, M. J.: First Simulations of
Designing Stratospheric Sulfate Aerosol Geoengineering to Meet Multiple Simultaneous Climate Objectives, Journal of Geophysical Research: Atmospheres, 122, 12,616–12,634, https://doi.org/10.1002/2017jd026874, 2017.

Kravitz, B., MacMartin, D. G., Tilmes, S., Richter, J. H., Mills, M. J., Cheng, W., Dagon, K., Glanville, A. S., Lamarque, J.-F., Simpson, I. R., Tribbia, J., and Vitt, F.: Comparing Surface and Stratospheric Impacts of Geoengineering With Different SO2 Injection Strategies, Journal of Geophysical Research: Atmospheres, 124, 7900–7918, https://doi.org/10.1029/2019JD030329, https://agupubs.onlinelibrary.
wiley.com/doi/abs/10.1029/2019JD030329, 2019.

Kravitz, B., MacMartin, D. G., Visioni, D., Boucher, O., Cole, J. N. S., Haywood, J., Jones, A., Lurton, T., Nabat, P., Niemeier, U., Robock, A., Séférian, R., and Tilmes, S.: Comparing different generations of idealized solar geoengineering simulations in the Geoengineering Model Intercomparison Project (GeoMIP), Atmospheric Chemistry and Physics Discussions, 2020, 1–31, https://doi.org/10.5194/acp-2020-732, https://acp.copernicus.org/preprints/acp-2020-732/, 2020.

Laakso, A., Snyder, P. K., Liess, S., Partanen, A.-I., and Millet, D. B.: Differing precipitation response between solar radiation management and carbon dioxide removal due to fast and slow components, Earth System Dynamics, 11, 415–434, https://doi.org/10.5194/esd-11-415-2020, https://esd.copernicus.org/articles/11/415/2020/, 2020.

Lee, W., MacMartin, D., Visioni, D., and Kravitz, B.: Expanding the design space of stratospheric aerosol geoengineering to include precipitation-based objectives and explore trade-offs, Earth System Dynamics, 11, 1051–1072, https://doi.org/10.5194/esd-11-1051-2020, https://esd.copernicus.org/articles/11/1051/2020/, 2020.

Lurton, T., Balkanski, Y., Bastrikov, V., Bekki, S., Bopp, L., Braconnot, P., Brockmann, P., Cadule, P., Contoux, C., Cozic, A., Cugnet, D., Dufresne, J.-L., Éthé, C., Foujols, M.-A., Ghattas, J., Hauglustaine, D., Hu, R.-M., Kageyama, M., Khodri, M., Lebas, N., Levavasseur, G., Marchand, M., Ottlé, C., Peylin, P., Sima, A., Szopa, S., Thiéblemont, R., Vuichard, N., and Boucher, O.: Implementation of the CMIP6 Forcing Data in the IPSL-CM6A-LR Model, Journal of Advances in Modeling Earth Systems, 12, e2019MS001 940, https://doi.org/10.1029/2019MS001940, https://agupubs.onlinelibrary.wiley.com/doi/abs/10.1029/2019MS001940, e2019MS001940 10.1029/2019MS001940, 2020.

Lutsko, N. J., Seeley, J. T., and Keith, D. W.: Estimating Impacts and Trade-offs in Solar Geoengineering Scenarios With a Moist Energy Balance Model, Geophysical Research Letters, 47, e2020GL087 290, https://doi.org/https://doi.org/10.1029/2020GL087290, https://agupubs.onlinelibrary.wiley.com/doi/abs/10.1029/2020GL087290, e2020GL087290 10.1029/2020GL087290, 2020.

MacMartin, D. G., Kravitz, B., and Rasch, P. J.: On solar geoengineering and climate uncertainty, Geophysical Research Letters, 42, 7156–7161, https://doi.org/10.1002/2015GL065391, 2015.

MacMartin, D. G., Kravitz, B., Mills, M. J., Tribbia, J. J., Tilmes, S., Richter, J. H., Vitt, F., and Lamarque, J.-F.: The Climate Response to Stratospheric Aerosol Geoengineering Can Be Tailored Using Multiple Injection Locations, Journal of Geophysical Research: Atmospheres, 122, 12,574–12,590, https://doi.org/10.1002/2017jd026868, 2017.

670 MacMartin, D. G., Ricke, K. L., and Keith, D. W.: Solar geoengineering as part of an overall strategy for meeting the 1.5°C Paris target, Philosophical Transactions of the Royal Society A: Mathematical, Physical and Engineering Sciences, 376, 20160 454, https://doi.org/10.1098/rsta.2016.0454, https://royalsocietypublishing.org/doi/abs/10.1098/rsta.2016.0454, 2018.

Marshall, L., Schmidt, A., Toohey, M., Carslaw, K. S., Mann, G. W., Sigl, M., Khodri, M., Timmreck, C., Zanchettin, D., Ball, W. T., Bekki, S., Brooke, J. S. A., Dhomse, S., Johnson, C., Lamarque, J.-F., LeGrande, A. N., Mills, M. J., Niemeier, U., Pope, J. O.,

675 Poulain, V., Robock, A., Rozanov, E., Stenke, A., Sukhodolov, T., Tilmes, S., Tsigaridis, K., and Tummon, F.: Multi-model comparison of the volcanic sulfate deposition from the 1815 eruption of Mt. Tambora, Atmospheric Chemistry and Physics, 18, 2307–2328, https://doi.org/10.5194/acp-18-2307-2018, https://acp.copernicus.org/articles/18/2307/2018/, 2018.

McCusker, K. E., Battisti, D. S., and Bitz, C. M.: Inability of stratospheric sulfate aerosol injections to preserve the West Antarctic Ice Sheet, Geophysical Research Letters, 42, 4989–4997, https://doi.org/https://doi.org/10.1002/2015GL064314, https://agupubs.onlinelibrary.wiley.com/doi/abs/10.1002/2015GL064314, 2015.

680

Meehl, G. A., Senior, C. A., Eyring, V., Flato, G., Lamarque, J.-F., Stouffer, R. J., Taylor, K. E., and Schlund, M.: Context for interpreting equilibrium climate sensitivity and transient climate response from the CMIP6 Earth system models, Science Advances, 6, https://doi.org/10.1126/sciadv.aba1981, https://advances.sciencemag.org/content/6/26/eaba1981, 2020.

Meinshausen, M., Nicholls, Z. R. J., Lewis, J., Gidden, M. J., Vogel, E., Freund, M., Beyerle, U., Gessner, C., Nauels, A., Bauer, N.,

685 Canadell, J. G., Daniel, J. S., John, A., Krummel, P. B., Luderer, G., Meinshausen, N., Montzka, S. A., Rayner, P. J., Reimann, S., Smith, S. J., van den Berg, M., Velders, G. J. M., Vollmer, M. K., and Wang, R. H. J.: The shared socio-economic pathway (SSP) greenhouse gas concentrations and their extensions to 2500, Geoscientific Model Development, 13, 3571–3605, https://doi.org/10.5194/gmd-13-3571-2020, https://gmd.copernicus.org/articles/13/3571/2020/, 2020.

Michou, M., Nabat, P., Saint-Martin, D., Bock, J., Decharme, B., Mallet, M., Roehrig, R., Séférian, R., Sénési, S., and Voldoire, A.:

690 Present-Day and Historical Aerosol and Ozone Characteristics in CNRM CMIP6 Simulations, Journal of Advances in Modeling Earth Systems, 12, e2019MS001 816, https://doi.org/https://doi.org/10.1029/2019MS001816, https://agupubs.onlinelibrary.wiley.com/doi/abs/10.1029/2019MS001816, e2019MS001816 10.1029/2019MS001816, 2020.

Muller, W. A., Jungclaus, J. H., Mauritsen, T., Baehr, J., Bittner, M., Budich, R., Bunzel, F., Esch, M., Ghosh, R., Haak, H., Ilyina, T., Kleine, T., Kornbluh, L., Li, H., Modali, K., Notz, D., Pohlmann, H., Roeckner, E., Stemmler, I., Tian, F., and Marotzke, J.: A Higher-

695 resolution Version of the Max Planck Institute Earth System Model (MPI-ESM1.2-HR), Journal of Advances in Modeling Earth Systems, 10, 1383–1413, https://doi.org/https://doi.org/10.1029/2017MS001217, 2018.

Niemeier, U. and Schmidt, H.: Changing transport processes in the stratosphere by radiative heating of sulfate aerosols, Atmospheric Chemistry and Physics, 17, 14 871–14 886, https://doi.org/10.5194/acp-17-14871-2017, https://www.atmos-chem-phys.net/17/14871/2017/, 2017.

700 Niemeier, U. and Timmreck, C.: What is the limit of climate engineering by stratospheric injection of SO2?, Atmospheric Chemistry and Physics, 15, 9129–9141, https://doi.org/10.5194/acp-15-9129-2015, https://www.atmos-chem-phys.net/15/9129/2015/, 2015.

Niemeier, U., Schmidt, H., Alterskjær, K., and Kristjánsson, J. E.: Solar irradiance reduction via climate engineering: Impact of different techniques on the energy balance and the hydrological cycle, Journal of Geophysical Research: Atmospheres, 118, 11,905–11,917, https://doi.org/10.1002/2013JD020445, https://agupubs.onlinelibrary.wiley.com/doi/abs/10.1002/2013JD020445, 2013.

705   Niemeier, U., Richter, J. H., and Tilmes, S.: Differing responses of the QBO to SO2 injections in two global models, Atmospheric Chemistry and Physics Discussions, 2020, 1–21, https://doi.org/10.5194/acp-2020-206, https://www.atmos-chem-phys-discuss.net/acp-2020-206/, 2020.

O'Neill, B. C., Tebaldi, C., van Vuuren, D. P., Eyring, V., Friedlingstein, P., Hurtt, G., Knutti, R., Kriegler, E., Lamarque, J.-F., Lowe, J., Meehl, G. A., Moss, R., Riahi, K., and Sanderson, B. M.: The Scenario Model Intercomparison Project (ScenarioMIP) for CMIP6,

710   Geoscientific Model Development, 9, 3461–3482, https://doi.org/10.5194/gmd-9-3461-2016, https://gmd.copernicus.org/articles/9/3461/2016/, 2016.

Parker, D. E., Wilson, H., Jones, P. D., Christy, J. R., and Folland, C. K.: The impact of mount Pinatubo on world-wide temperatures, International Journal of Climatology, 16, 487–497, https://doi.org/https://doi.org/10.1002/(SICI)1097-0088(199605)16:5<487::AID-JOC39>3.0.CO;2-J, 1996.

715   Pendergrass, A. G. and Hartmann, D. L.: The Atmospheric Energy Constraint on Global-Mean Precipitation Change, Journal of Climate, 27, 757–768, https://doi.org/10.1175/JCLI-D-13-00163.1, https://doi.org/10.1175/JCLI-D-13-00163.1, 2014.

Pierce, J. R., Weisenstein, D. K., Heckendorn, P., Peter, T., and Keith, D. W.: Efficient formation of stratospheric aerosol for climate engineering by emission of condensible vapor from aircraft, Geophysical Research Letters, 37, https://doi.org/10.1029/2010GL043975, https://agupubs.onlinelibrary.wiley.com/doi/abs/10.1029/2010GL043975, 2010.

720   Pitari, G., Aquila, V., Kravitz, B., Robock, A., Watanabe, S., Cionni, I., Luca, N. D., Genova, G. D., Mancini, E., and Tilmes, S.: Stratospheric ozone response to sulfate geoengineering: Results from the Geoengineering Model Intercomparison Project (GeoMIP), Journal of Geophysical Research: Atmospheres, 119, 2629–2653, https://doi.org/10.1002/2013JD020566, https://agupubs.onlinelibrary.wiley.com/doi/abs/10.1002/2013JD020566, 2014.

Pitari, G., Genova, G. D., Mancini, E., Visioni, D., Gandolfi, I., and Cionni, I.: Stratospheric aerosols from major volcanic eruptions: A

725   composition-climate model study of the aerosol cloud dispersal and e-folding time, Atmosphere, https://doi.org/10.3390/atmos7060075, http://www.scopus.com/inward/record.url?eid=2-s2.0-84976884421{&}partnerID=MN8TOARS, 2016.

Plazzotta, M., Séférian, R., Douville, H., Kravitz, B., and Tjiputra, J.: Land Surface Cooling Induced by Sulfate Geoengineering Constrained by Major Volcanic Eruptions, Geophysical Research Letters, 45, 5663–5671, https://doi.org/https://doi.org/10.1029/2018GL077583, https://agupubs.onlinelibrary.wiley.com/doi/abs/10.1029/2018GL077583, 2018.

730   Plazzotta, M., Séférian, R., and Douville, H.: Impact of Solar Radiation Modification on Allowable CO2 Emissions: What Can We Learn From Multimodel Simulations?, Earth's Future, 7, 664–676, https://doi.org/https://doi.org/10.1029/2019EF001165, https://agupubs.onlinelibrary.wiley.com/doi/abs/10.1029/2019EF001165, 2019.

Richter, J. H., Tilmes, S., Mills, M. J., Tribbia, J. J., Kravitz, B., Macmartin, D. G., Vitt, F., and Lamarque, J. F.: Stratospheric dynamical response and ozone feedbacks in the presence of SO2 injections, Journal of Geophysical Research: Atmospheres, 122, 12,557–12,573,

735   https://doi.org/10.1002/2017JD026912, 2017.

Robock, A.: Volcanic eruptions and climate, Reviews of Geophysics, 38, 191–219, https://doi.org/10.1029/1998RG000054, https://agupubs.onlinelibrary.wiley.com/doi/abs/10.1029/1998RG000054, 2000.

Russotto, R. D. and Ackerman, T. P.: Changes in clouds and thermodynamics under solar geoengineering and implications for required solar reduction, Atmospheric Chemistry and Physics, 18, 11 905–11 925, https://doi.org/10.5194/acp-18-11905-2018, https://www.

740   atmos-chem-phys.net/18/11905/2018/, 2018a.

Russotto, R. D. and Ackerman, T. P.: Energy transport, polar amplification, and ITCZ shifts in the GeoMIP G1 ensemble, Atmospheric Chemistry and Physics, 18, 2287–2305, https://doi.org/10.5194/acp-18-2287-2018, https://www.atmos-chem-phys.net/18/2287/2018/, 2018b.

Seeley, J. T., Lutsko, N. J., and Keith, D. W.: Designing a Radiative Antidote to CO2, Geophysical Research Letters, 48, https://doi.org/https://doi.org/10.1029/2020GL090876, https://agupubs.onlinelibrary.wiley.com/doi/abs/10.1029/2020GL090876, 2021.

745 Seferian, R.: CNRM-CERFACS CNRM-ESM2-1 model output prepared for CMIP6 CMIP, https://doi.org/10.22033/ESGF/CMIP6.1391, https://doi.org/10.22033/ESGF/CMIP6.1391, 2018.

Séférian, R., Berthet, S., Yool, A., Palmiéri, J., Bopp, L., Tagliabue, A., Kwiatkowski, L., Aumont, O., Christian, J., Dunne, J., Gehlen, M., Ilyina, T., John, J. G., Li, H., Long, M. C., Luo, J. Y., Nakano, H., Romanou, A., Schwinger, J., Stock, C., Santana-Falcón, Y., Takano, Y., Tjiputra, J., Tsujino, H., Watanabe, M., Wu, T., Wu, F., and Yamamoto, A.: Tracking Improvement in Simulated Marine Biogeochemistry
750 Between CMIP5 and CMIP6, Current Climate Change Reports, 6, 95–119, 2020.

Sellar, A. A., Jones, C. G., Mulcahy, J. P., Tang, Y., Yool, A., Wiltshire, A., O'Connor, F. M., Stringer, M., Hill, R., Palmieri, J., Woodward, S., de Mora, L., Kuhlbrodt, T., Rumbold, S. T., Kelley, D. I., Ellis, R., Johnson, C. E., Walton, J., Abraham, N. L., Andrews, M. B., Andrews, T., Archibald, A. T., Berthou, S., Burke, E., Blockley, E., Carslaw, K., Dalvi, M., Edwards, J., Folberth, G. A., Gedney, N., Griffiths, P. T., Harper, A. B., Hendry, M. A., Hewitt, A. J., Johnson, B., Jones, A., Jones, C. D., Keeble, J., Liddicoat, S., Morgenstern,
755 O., Parker, R. J., Predoi, V., Robertson, E., Siahaan, A., Smith, R. S., Swaminathan, R., Woodhouse, M. T., Zeng, G., and Zerroukat, M.: UKESM1: Description and Evaluation of the U.K. Earth System Model, Journal of Advances in Modeling Earth Systems, 11, 4513–4558, https://doi.org/10.1029/2019MS001739, https://agupubs.onlinelibrary.wiley.com/doi/abs/10.1029/2019MS001739, 2019.

Sherwood, S., Webb, M. J., Annan, J. D., Armour, K. C., Forster, P. M., Hargreaves, J. C., Hegerl, G., Klein, S. A., Marvel, K. D., Rohling, E. J., Watanabe, M., Andrews, T., Braconnot, P., Bretherton, C. S., Foster, G. L., Hausfather, Z., Heydt, A. S. v. d., Knutti, R., Mauritsen,
760 T., Norris, J. R., Proistosescu, C., Rugenstein, M., Schmidt, G. A., Tokarska, K. B., and Zelinka, M. D.: An assessment of Earth's climate sensitivity using multiple lines of evidence, Reviews of Geophysics, n/a, e2019RG000 678, https://doi.org/10.1029/2019RG000678, https://agupubs.onlinelibrary.wiley.com/doi/abs/10.1029/2019RG000678, e2019RG000678 2019RG000678, 2020.

Simpson, I., Tilmes, S., Richter, J., Kravitz, B., MacMartin, D., Mills, M., Fasullo, J., and Pendergrass, A.: The regional hydroclimate response to stratospheric sulfate geoengineering and the role of stratospheric heating, Journal of Geophysical Research: Atmospheres, p.
765 2019JD031093, https://doi.org/10.1029/2019JD031093, https://onlinelibrary.wiley.com/doi/abs/10.1029/2019JD031093, 2019.

Soden, B. J., Wetherald, R. T., Stenchikov, G. L., and Robock, A.: Global Cooling After the Eruption of Mount Pinatubo: A Test of Climate Feedback by Water Vapor, Science, 296, 727–730, https://doi.org/10.1126/science.296.5568.727, https://science.sciencemag.org/content/296/5568/727, 2002.

Stockhause, M. and Lautenschlager, M.: CMIP6 Data Citation of Evolving Data, Data Science Journal, 16, 30,
770 https://doi.org/http://doi.org/10.5334/dsj-2017-030, 2021.

Séférian, R., Nabat, P., Michou, M., Saint-Martin, D., Voldoire, A., Colin, J., Decharme, B., Delire, C., Berthet, S., Chevallier, M., Sénési, S., Franchisteguy, L., Vial, J., Mallet, M., Joetzjer, E., Geoffroy, O., Guérémy, J.-F., Moine, M.-P., Msadek, R., Ribes, A., Rocher, M., Roehrig, R., Salas-y Mélia, D., Sanchez, E., Terray, L., Valcke, S., Waldman, R., Aumont, O., Bopp, L., Deshayes, J., Éthé, C., and Madec, G.: Evaluation of CNRM Earth System Model, CNRM-ESM2-1: Role of Earth System Processes in Present-Day and Future Climate,
775 Journal of Advances in Modeling Earth Systems, 11, 4182–4227, https://doi.org/10.1029/2019MS001791, https://agupubs.onlinelibrary.wiley.com/doi/abs/10.1029/2019MS001791, 2019.

Tang, Y., Rumbold, S., Ellis, R., Kelley, D., Mulcahy, J., Sellar, A., Walton, J., and Jones, C.: MOHC UKESM1.0-LL model output prepared for CMIP6 CMIP historical, https://doi.org/10.22033/ESGF/CMIP6.6113, https://doi.org/10.22033/ESGF/CMIP6.6113, 2019.

Thornhill, G., Collins, W., Olivié, D., Skeie, R. B., Archibald, A., Bauer, S., Checa-Garcia, R., Fiedler, S., Folberth, G., Gjermundsen, A.,
780 Horowitz, L., Lamarque, J.-F., Michou, M., Mulcahy, J., Nabat, P., Naik, V., O'Connor, F. M., Paulot, F., Schulz, M., Scott, C. E., Séférian,

R., Smith, C., Takemura, T., Tilmes, S., Tsigaridis, K., and Weber, J.: Climate-driven chemistry and aerosol feedbacks in CMIP6 Earth system models, Atmospheric Chemistry and Physics, 21, 1105–1126, 2021.

Tilmes, S., Fasullo, J., Lamarque, J.-F., Marsh, D. R., Mills, M., Alterskjær, K., Muri, H., Kristjánsson, J. E., Boucher, O., Schulz, M., Cole, J. N. S., Curry, C. L., Jones, A., Haywood, J., Irvine, P. J., Ji, D., Moore, J. C., Karam, D. B., Kravitz, B., Rasch, P. J., Singh, B., Yoon, J.-H., Niemeier, U., Schmidt, H., Robock, A., Yang, S., and Watanabe, S.: The hydrological impact of geoengineering in the Geoengineering Model Intercomparison Project (GeoMIP), Journal of Geophysical Research: Atmospheres, 118, 11,036–11,058, https://doi.org/10.1002/jgrd.50868, https://agupubs.onlinelibrary.wiley.com/doi/abs/10.1002/jgrd.50868, 2013.

Tilmes, S., Mills, M. J., Niemeier, U., Schmidt, H., Robock, A., Kravitz, B., Lamarque, J.-F., Pitari, G., and English, J. M.: A new Geoengineering Model Intercomparison Project (GeoMIP) experiment designed for climate and chemistry models, Geoscientific Model Development, 8, 43–49, https://doi.org/10.5194/gmd-8-43-2015, https://gmd.copernicus.org/articles/8/43/2015/, 2015.

Tilmes, S., Richter, J. H., Kravitz, B., Macmartin, D. G., Mills, M. J., Simpson, I. R., Glanville, A. S., Fasullo, J. T., Phillips, A. S., Lamarque, J. F., Tribbia, J., Edwards, J., Mickelson, S., and Ghosh, S.: CESM1(WACCM) stratospheric aerosol geoengineering large ensemble project, Bulletin of the American Meteorological Society, pp. 2361–2371, https://doi.org/10.1175/BAMS-D-17-0267.1, 2018a.

Tilmes, S., Richter, J. H., Mills, M. J., Kravitz, B., MacMartin, D. G., Garcia, R. R., Kinnison, D. E., Lamarque, J. F., Tribbia, J., and Vitt, F.: Effects of Different Stratospheric SO2 Injection Altitudes on Stratospheric Chemistry and Dynamics, Journal of Geophysical Research: Atmospheres, 123, 4654–4673, https://doi.org/10.1002/2017JD028146, 2018b.

Tilmes, S., MacMartin, D. G., Lenaerts, J. T. M., van Kampenhout, L., Muntjewerf, L., Xia, L., Harrison, C. S., Krumhardt, K. M., Mills, M. J., Kravitz, B., and Robock, A.: Reaching 1.5 and 2.0C global surface temperature targets using stratospheric aerosol geoengineering, Earth System Dynamics, 11, 579–601, https://doi.org/10.5194/esd-11-579-2020, https://esd.copernicus.org/articles/11/579/2020/, 2020.

Timmreck, C., Mann, G. W., Aquila, V., Hommel, R., Lee, L. A., Schmidt, A., Brühl, C., Carn, S., Chin, M., Dhomse, S. S., Diehl, T., English, J. M., Mills, M. J., Neely, R., Sheng, J., Toohey, M., and Weisenstein, D.: The Interactive Stratospheric Aerosol Model Intercomparison Project (ISA-MIP): motivation and experimental design, Geoscientific Model Development, 11, 2581–2608, https://doi.org/10.5194/gmd-11-2581-2018, https://gmd.copernicus.org/articles/11/2581/2018/, 2018.

Visioni, D., Pitari, G., and Aquila, V.: Sulfate geoengineering: A review of the factors controlling the needed injection of sulfur dioxide, Atmospheric Chemistry and Physics, https://doi.org/10.5194/acp-17-3879-2017, 2017a.

Visioni, D., Pitari, G., Aquila, V., Tilmes, S., Cionni, I., Di Genova, G., and Mancini, E.: Sulfate geoengineering impact on methane transport and lifetime: results from the Geoengineering Model Intercomparison Project (GeoMIP), Atmospheric Chemistry and Physics, 17, 11 209–11 226, https://doi.org/10.5194/acp-17-11209-2017, https://www.atmos-chem-phys.net/17/11209/2017/, 2017b.

Visioni, D., Pitari, G., Di Genova, G., Tilmes, S., and Cionni, I.: Upper tropospheric ice sensitivity to sulfate geoengineering, Atmospheric Chemistry and Physics, https://doi.org/10.5194/acp-18-14867-2018, 2018a.

Visioni, D., Pitari, G., Tuccella, P., and Curci, G.: Sulfur deposition changes under sulfate geoengineering conditions: Quasi-biennial oscillation effects on the transport and lifetime of stratospheric aerosols, Atmospheric Chemistry and Physics, https://doi.org/10.5194/acp-18-2787-2018, 2018b.

Visioni, D., MacMartin, D. G., Kravitz, B., Tilmes, S., Mills, M. J., Richter, J. H., and Boudreau, M. P.: Seasonal Injection Strategies for Stratospheric Aerosol Geoengineering, Geophysical Research Letters, 46, 7790–7799, https://doi.org/10.1029/2019GL083680, https://agupubs.onlinelibrary.wiley.com/doi/abs/10.1029/2019GL083680, 2019.

Visioni, D., MacMartin, D. G., Kravitz, B., Lee, W., Simpson, I. R., and Richter, J. H.: Reduced poleward transport due to stratospheric heating under stratospheric aerosols geoengineering, Geophysical Research Letters, n/a, e2020GL089 470,

https://doi.org/10.1029/2020GL089470, https://agupubs.onlinelibrary.wiley.com/doi/abs/10.1029/2020GL089470, e2020GL089470 2020GL089470, 2020a.

Visioni, D., MacMartin, D. G., Kravitz, B., Richter, J. H., Tilmes, S., and Mills, M. J.: Seasonally Modulated Stratospheric Aerosol Geo-engineering Alters the Climate Outcomes, Geophysical Research Letters, n/a, e2020GL088 337, https://doi.org/10.1029/2020GL088337, https://agupubs.onlinelibrary.wiley.com/doi/abs/10.1029/2020GL088337, e2020GL088337 2020GL088337, 2020b.

Visioni, D., MacMartin, D. G., and Kravitz, B.: Is Turning Down the Sun a Good Proxy for Stratospheric Sulfate Geoengineering?, Journal of Geophysical Research: Atmospheres, n/a, e2020JD033 952, https://doi.org/https://doi.org/10.1029/2020JD033952, https://agupubs.onlinelibrary.wiley.com/doi/abs/10.1029/2020JD033952, e2020JD033952 2020JD033952, 2021.

Wieners, K.-H., Giorgetta, M., Jungclaus, J., Reick, C., Esch, M., Bittner, M., Legutke, S., Schupfner, M., Wachsmann, F., Gayler, V., Haak, H., de Vrese, P., Raddatz, T., Mauritsen, T., von Storch, J.-S., Behrens, J., Brovkin, V., Claussen, M., Crueger, T., Fast, I., Fiedler, S., Hagemann, S., Hohenegger, C., Jahns, T., Kloster, S., Kinne, S., Lasslop, G., Kornblueh, L., Marotzke, J., Matei, D., Meraner, K., Mikolajewicz, U., Modali, K., Müller, W., Nabel, J., Notz, D., Peters, K., Pincus, R., Pohlmann, H., Pongratz, J., Rast, S., Schmidt, H., Schnur, R., Schulzweida, U., Six, K., Stevens, B., Voigt, A., and Roeckner, E.: MPI-M MPI-ESM1.2-LR model output prepared for CMIP6 CMIP historical, https://doi.org/10.22033/ESGF/CMIP6.6595, https://doi.org/10.22033/ESGF/CMIP6.6595, 2019.

Xia, L., Nowack, P. J., Tilmes, S., and Robock, A.: Impacts of stratospheric sulfate geoengineering on tropospheric ozone, Atmospheric Chemistry and Physics, 17, 11 913–11 928, https://doi.org/10.5194/acp-17-11913-2017, https://www.atmos-chem-phys.net/17/11913/2017/, 2017.

Zarnetske, P. L., Gurevitch, J., Franklin, J., Groffman, P., Harrison, C., Hellmann, J., Hoffman, F. M., Kothari, S., Robock, A., Tilmes, S., Visioni, D., Wu, J., Xia, L., and Yang, C.-E.: Potential ecological impacts of climate intervention by reflecting sunlight to cool Earth: Ecological impacts of climate intervention, Proceeding of the National Academy of Science, In press, n/a, 2021.

Zelinka, M. D., Myers, T. A., McCoy, D. T., Po-Chedley, S., Caldwell, P. M., Ceppi, P., Klein, S. A., and Taylor, K. E.: Causes of Higher Climate Sensitivity in CMIP6 Models, Geophysical Research Letters, 47, e2019GL085 782, https://doi.org/10.1029/2019GL085782, https://agupubs.onlinelibrary.wiley.com/doi/abs/10.1029/2019GL085782, e2019GL085782 10.1029/2019GL085782, 2020.